BERKELEY LAB
Bringing Science Solutions to the World

U.S. DEPARTMENT OF ENERGY
Office of Science

GMn (Preliminary) Results

Provakar Datta
(for the GMn team)

Representing the SBS-GMn and -nTPE Graduate Students: Vanessa Brio (Catania U.), John Boyd (UVA), Provakar Datta (UConn), Nathaniel Lashley-Colthirst (Hampton U.), Ralph Marinaro (University of Glasgow), Anuruddha Rathnayake (UVA), Maria Satnik (W&M), Sebastian Seeds (UConn), Ezekiel Wertz (W&M)

Jefferson Lab
Exploring the Nature of Matter

SUPER BIGBITE SPECTROMETER

Outline

- Nucleon Form Factors and the Structure of the Nucleon
- A Brief Overview of the SBS-GMn Experiment
- Physics Analysis Methodology, Challenges, and Preliminary Results
- Status of 3rd Reconstruction Pass – The Last Step to Finalize Results
- Summary and outlook

Elastic eN Scattering and Nucleon Form Factors

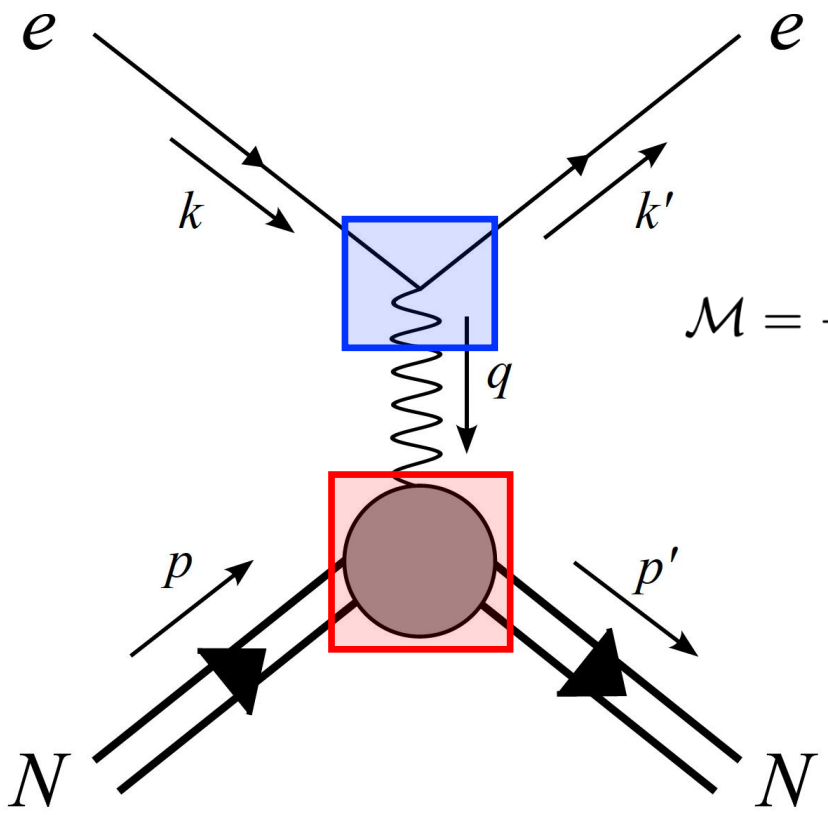

❖ Scattering Amplitude:

$$\mathcal{M} = -\frac{4\pi\alpha}{Q^2}\,\bar{u}^{s'}(k')\gamma^{\mu}u^{s}(k)\,\bar{u}^{r'}(p')\left[\gamma_{\mu}F_1^N(Q^2) + \frac{i\sigma_{\mu\nu}q^{\nu}}{2M}F_2^N(Q^2)\right]u^{r}(p)$$

Leptonic Vertex

Hadronic Vertex

$F_1^N \Rightarrow$ Dirac Form Factor

$F_2^N \Rightarrow$ Pauli Form Factor

$N \Rightarrow$ Proton (p), Neutron (n)

$Q^2 = -q^2 = (k - k')^2$

Figure: Elastic eN scattering in OPE Approximation

Introducing Sachs Form Factors

Sachs Electric Form Factor

$$G_E^N(Q^2) = F_1^N(Q^2) - \tau_N F_2^N(Q^2)$$

$$G_M^N(Q^2) = F_1^N(Q^2) + F_2^N(Q^2)$$

Sachs Magnetic Form Factor

❖ Normalization:

$$\text{At } Q^2 = 0, \begin{cases} G_E^p(0) = 1, & G_M^p(0) = \mu_p \\ G_E^n(0) = 0, & G_M^n(0) = \mu_n \end{cases}$$

❖ Differential Cross Section in OPE Approx. (Rosenbluth Formula):

$$\frac{d\sigma}{d\Omega} = \frac{\sigma_{\text{Mott}}\epsilon_N}{1+\tau_N}\left(\epsilon_N G_E^{N\,2}(Q^2) + \tau_N G_M^{N\,2}(Q^2)\right)$$

- $\tau_N = Q^2/4M_N^2$
- $\epsilon_N = (1 + 2(1+\tau_N)\tan^2(\theta_e/2))^{-1}$

Electromagnetic Form Factors & Nucleon Imaging

- In non-relativistic limit G_E and G_M are related to the 3D Fourier transforms of the spatial charge and current distributions within the nucleon, respectively. But relativistic corrections are large and model dependent.

- However, in the infinite momentum frame (IMF), a **model-independent** density interpretation can be drawn in terms of transverse distributions by relating the form factors to Generalized Parton Distribution (GPD) moments.

Transverse charge density of Longitudinally Polarized **Proton**

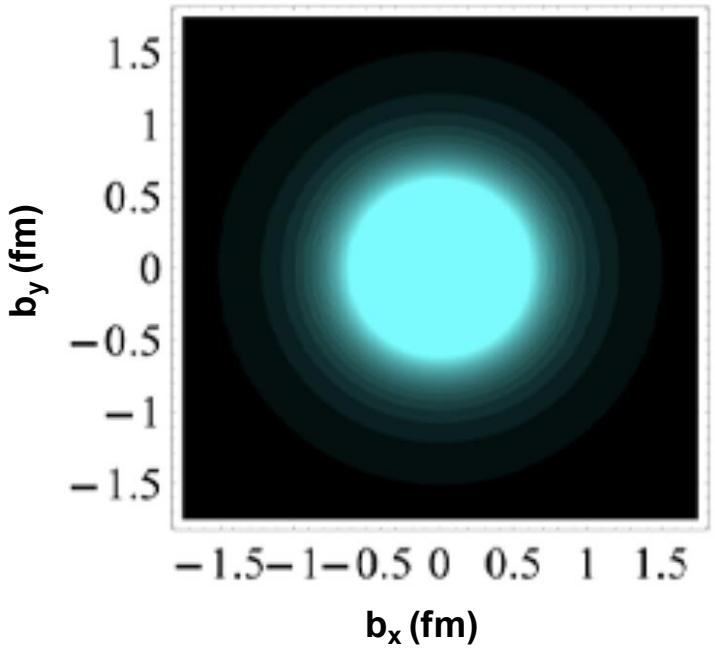

Transverse charge density of Longitudinally Polarized **Neutron**

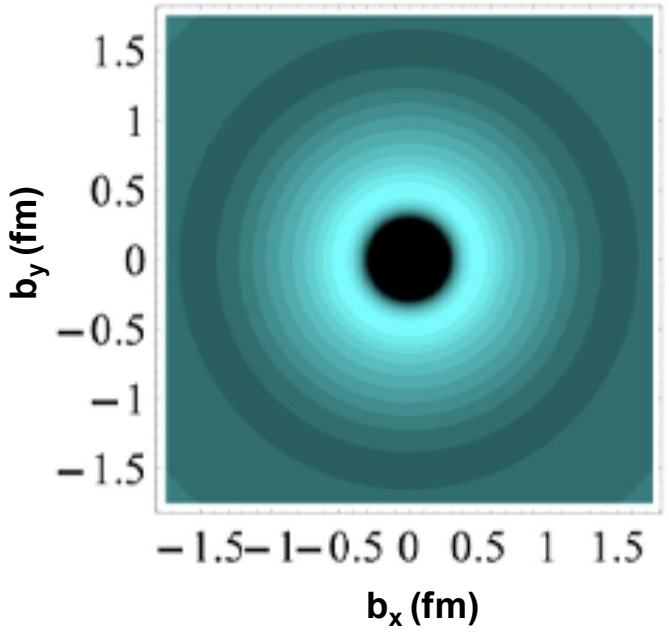

Ref: Carlson *et al*: Phys. Rev. Lett. 100, 032004 (2008)

Outline

- Nucleon Form Factors and the Structure of the Nucleon
- A Brief Overview of the SBS-GMn Experiment
- Physics Analysis Methodology, Challenges, and Preliminary Results
- Status of 3rd Reconstruction Pass – The Last Step to Finalize Results
- Summary and outlook

SBS-GMn Experiment, Fall 2021 – Feb 2022

Q^2 increase: 6 → 13.5 (GeV/c)²

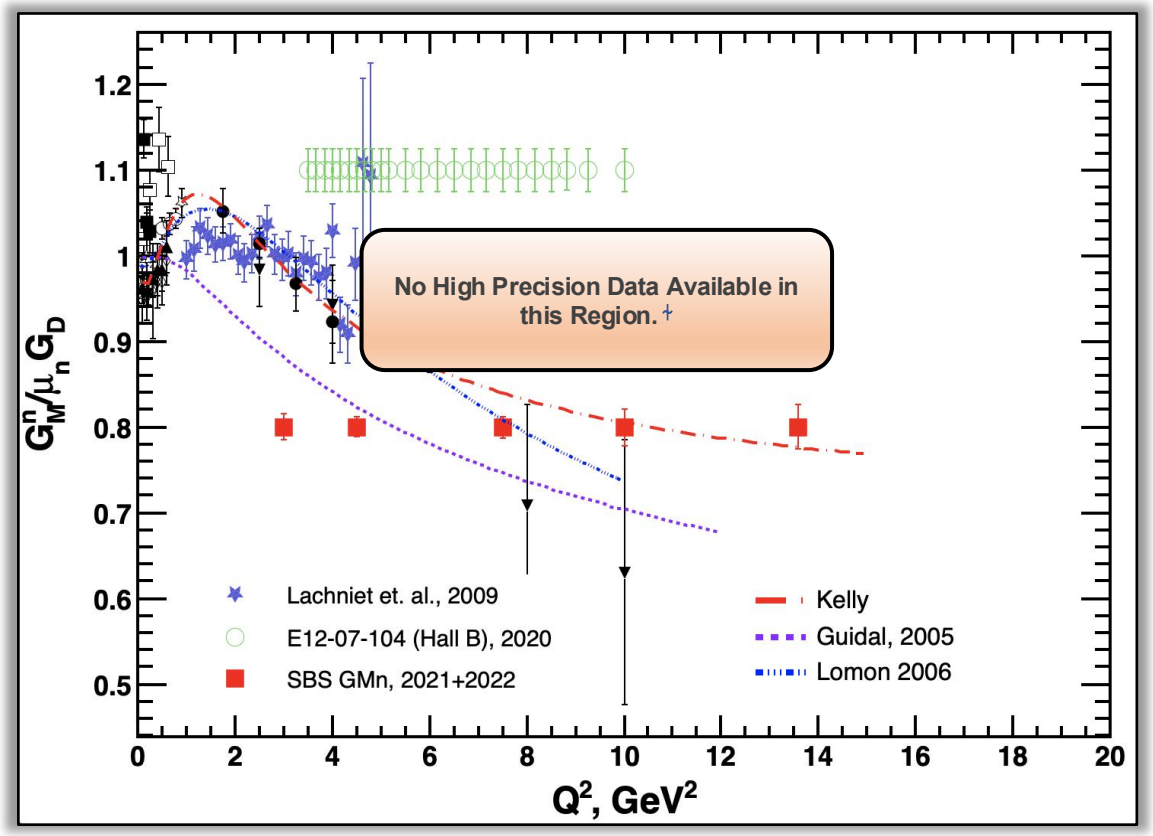

SBS-GMn (E12-09-019) took data in Jefferson Lab's Hall A from Fall 2021 to February 2022.

- **Goal:**
  - High precision measurement of neutron magnetic form factor (G_M^n) at unprecedented Q^2.
- **Challenges:**
  - Elastic eN scattering cross-section falls like $1/Q^{12}$!!
  - High precision tracking at very high rates.
  - Simultaneous detection of high energy nucleons with high and comparable efficiencies.

The Super BigBite Spectrometer – Design Highlights

SBS Dipole Magnet

- $1.6\ \mathrm{Tm}$ field integral
- $50\ msr$ solid angle acceptance at $15°$ (Achieved with a cut in the yoke for passage of the beam line)
- Separates high energy nucleons by charge

Hadron Calorimeter (HCAL)

- $2 \times 3.7\ \mathrm{m}^2$ active area
- Detects both the nucleons with high & comparable efficiencies
- $\approx 5\ \mathrm{cm}$ position resolution
- $\approx 1.2\ \mathrm{ns}$ time resolution

Gas Electron Multiplier (GEM) Tracker

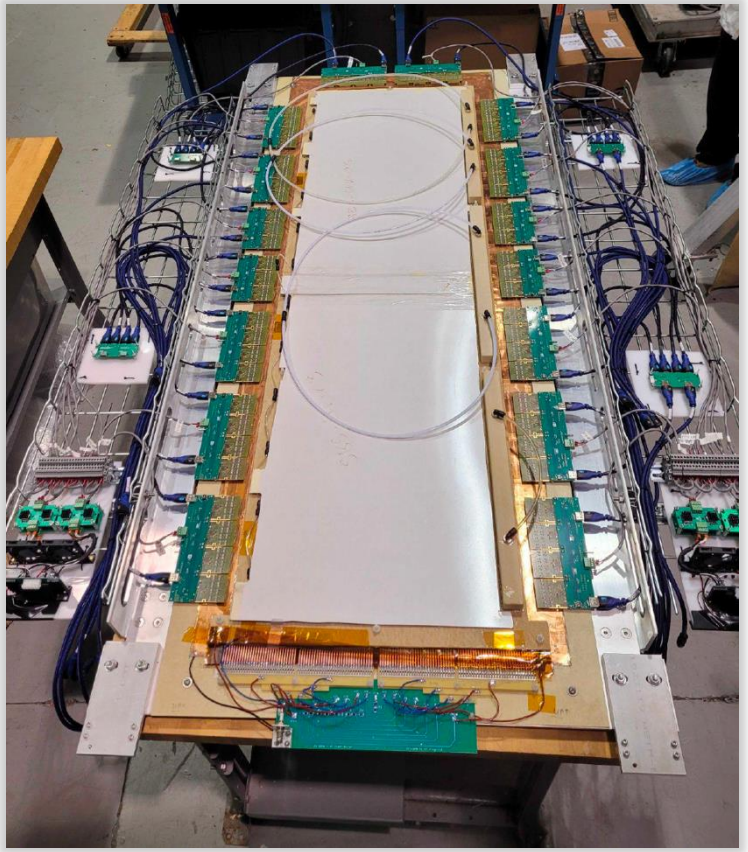

- $50 \times 150\ \mathrm{cm}^2$ active area
- $\approx 70\ \mu\mathrm{m}$ position resolution
- Capable of handling hundreds of kHz rates per cm^2.

BigBite and Super BigBite Spectrometers in Hall A

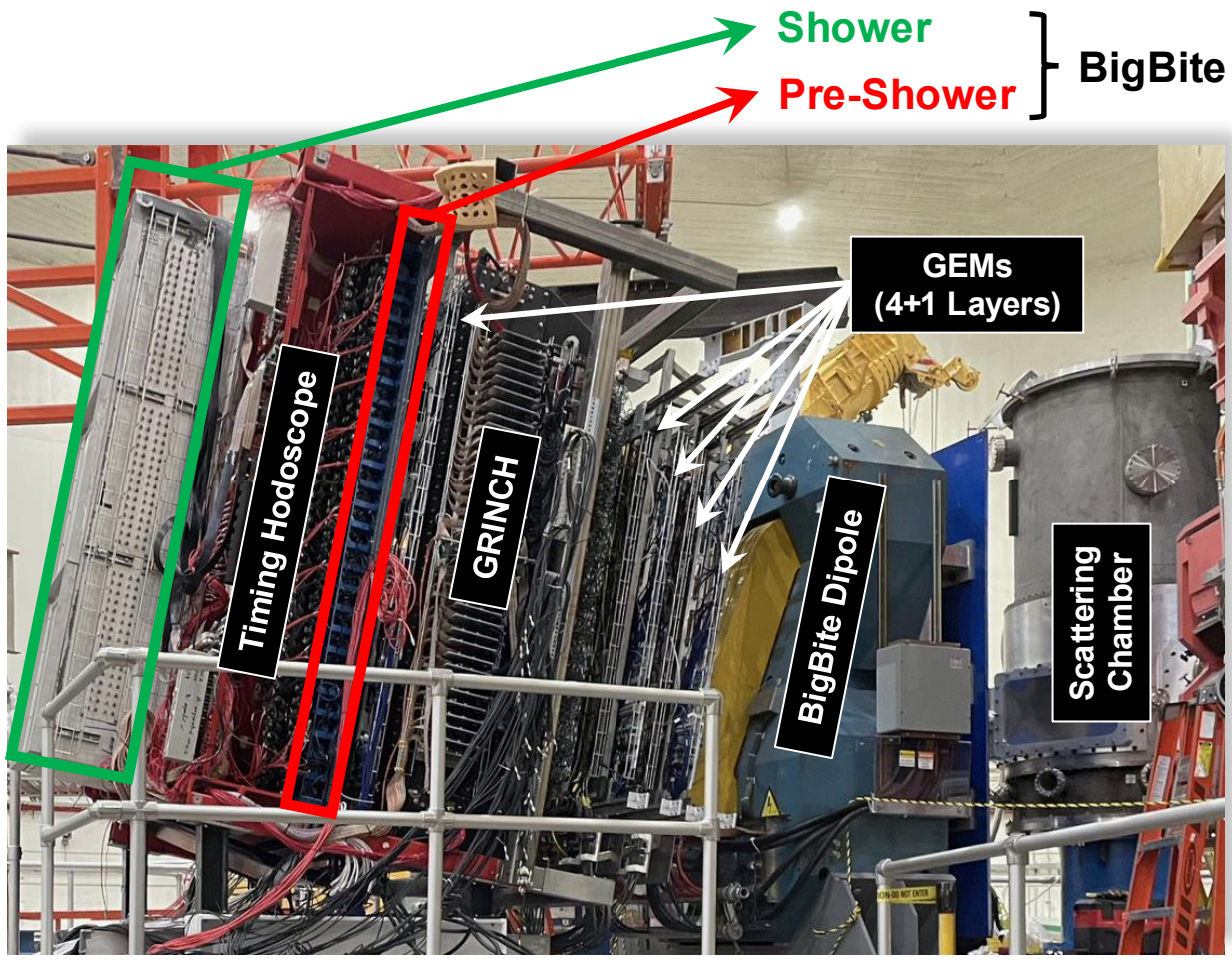

Electron Arm: The BigBite Spectrometer (Side View)

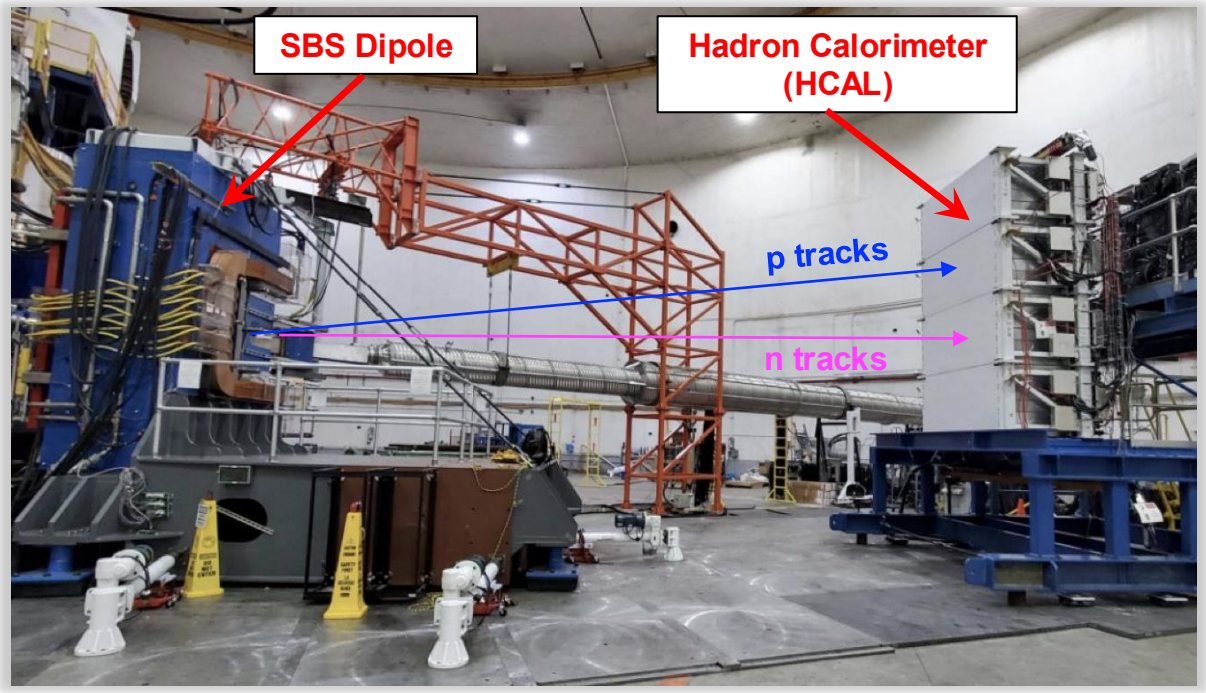

Hadron Arm: The Super BigBite Spectrometer

Outline

- Nucleon Form Factors and the Structure of the Nucleon
- A Brief Overview of the SBS-GMn Experiment
- Physics Analysis Methodology, Challenges, and Preliminary Results
- Status of 3rd Reconstruction Pass – The Last Step to Finalize Results
- Summary and outlook

SBS-GMn Measurement Technique ("Ratio Method")

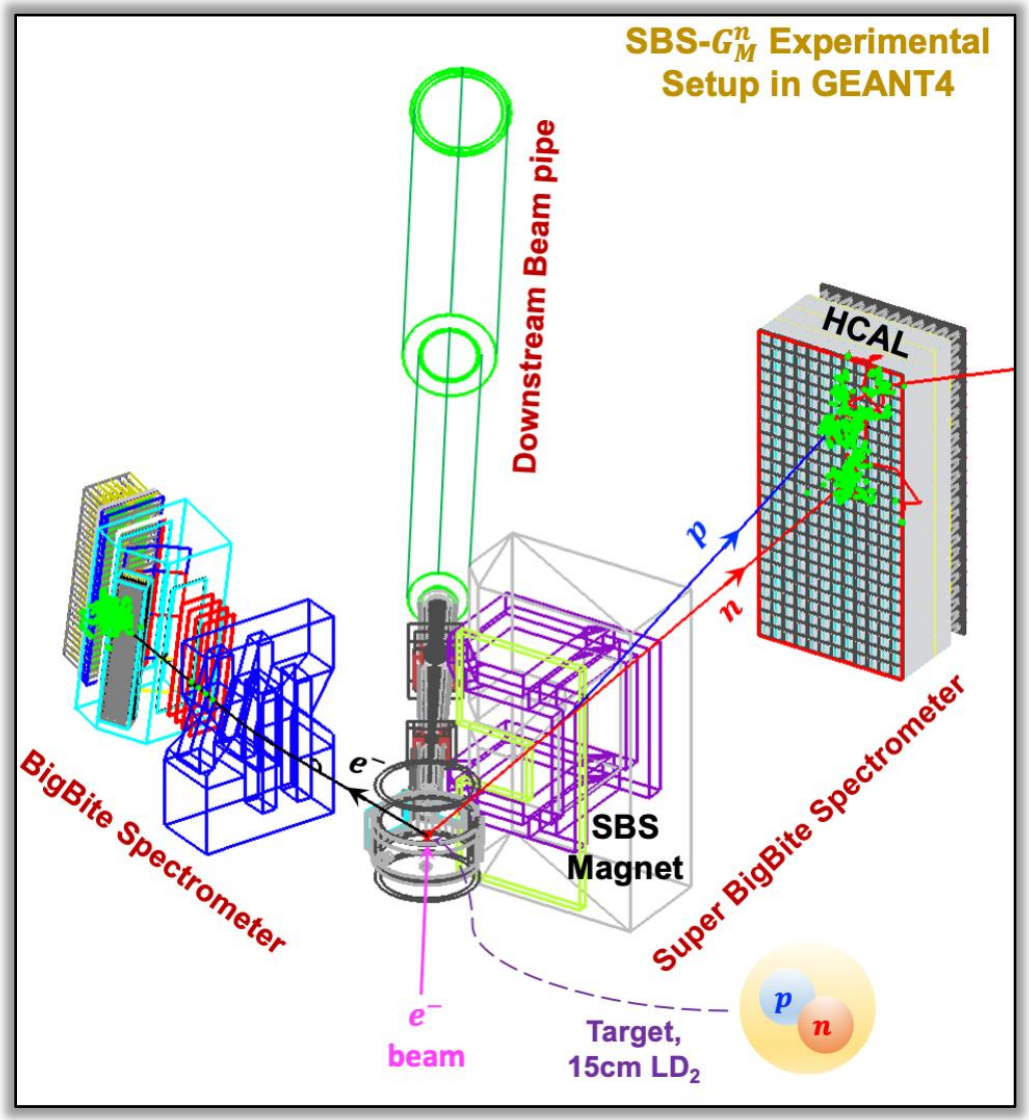

- Simultaneous detection of electrons and nucleons lets us use "ratio method"[1], which offers significant cancellation of some systematic errors.

- 3 major steps to get G_M^n:

1. Extracting QE cross section ratio, R^{QE}, directly from the experiment:

$$R^{QE} = \frac{\frac{d\sigma}{d\Omega}\Big|_{D(e,e'n)}}{\frac{d\sigma}{d\Omega}\Big|_{D(e,e'p)}}$$

2. Apply radiative and nuclear corrections to obtain:

$$R = \frac{\frac{d\sigma}{d\Omega}\Big|_{n(e,e')}}{\frac{d\sigma}{d\Omega}\Big|_{p(e,e')}} = \frac{\frac{\sigma_{\mathrm{Mott}}\epsilon_n}{1+\tau_n}\left(\epsilon_n G_E^{n\,2} + \tau_n G_M^{n\,2}\right)}{\frac{\sigma_{\mathrm{Mott}}\epsilon_p}{1+\tau_p}\sigma_{Red}^{p}}$$

3. Finally,

$$G_M^n = -\left[\frac{1}{\tau_n}\frac{\epsilon_n(1+\tau_n)}{\epsilon_p(1+\tau_p)}\sigma_{Red}^{p} R - \frac{\epsilon_n}{\tau_n}G_E^{n\,2}\right]^{\frac{1}{2}}$$

[1] L. Durand, Phys. Rev. 115 1020 (1959).

Kinematics of SBS-GMn

Table 1: Kinematics of SBS-GMn. Q^2 is the central Q^2, E_{beam} is the beam energy, θ_{BB} is the BigBite central angle, θ_{SBS} is the Super BigBite central angle, ϵ is the longitudinal polarization of the virtual photon, $E_{e'}$ is the average scattered electron energy, and $E_{p'}$ is the average scattered proton energy.

Q^2 (GeV/c)^2	ϵ	E_{beam} (GeV)	θ_{BB} (deg)	θ_{SBS} (deg)	$E_{e'}$ (GeV)	$E_{p'}$ (GeV)
3.0	**0.72**	3.73	36.0	31.9	2.12	2.4
4.5	**0.51**	4.03	49.0	22.5	1.63	3.2
4.5	**0.80**	5.98	26.5	29.9	3.58	3.2
7.4	**0.46**	5.97	46.5	17.3	2.00	4.8
9.9	**0.50**	7.91	40.0	16.1	2.66	6.1
13.5	**0.41**	9.86	42.0	13.3	2.67	8.1

- Data was collected at five different Q^2 points for G_M^n extraction.
- The high ϵ data at 4.5 GeV^2 is dedicated to the SBS-nTPE (E12-20-010) experiment, which aims to do first high precision Rosenbluth separation of the neutron form factors to shed some light on the two-photon exchange (TPE) contribution in the elastic en scattering. Stay tuned for Zeke's talk!

Detector Performance Highlights (from 2nd Pass Reconstruction)

- **BigBite Spectrometer:**
  - Momentum resolution $\left(\frac{\sigma_p}{p}\right)$: $\mathbf{1-1.5\%}$
  - Angular resolution (in-plane & out-of-plane): $\mathbf{1-2}$ **mrad**
  - Vertex resolution: $\mathbf{2-6}$ **mm**

- **Super BigBite Spectrometer:**
  - Hadron Calorimeter (HCAL):
    - Time Resolution: $\mathbf{1.2-1.3}$ **ns**
    - Position Resolution: $\mathbf{5-6}$ **cm**

❖ These are in line with our expectations.

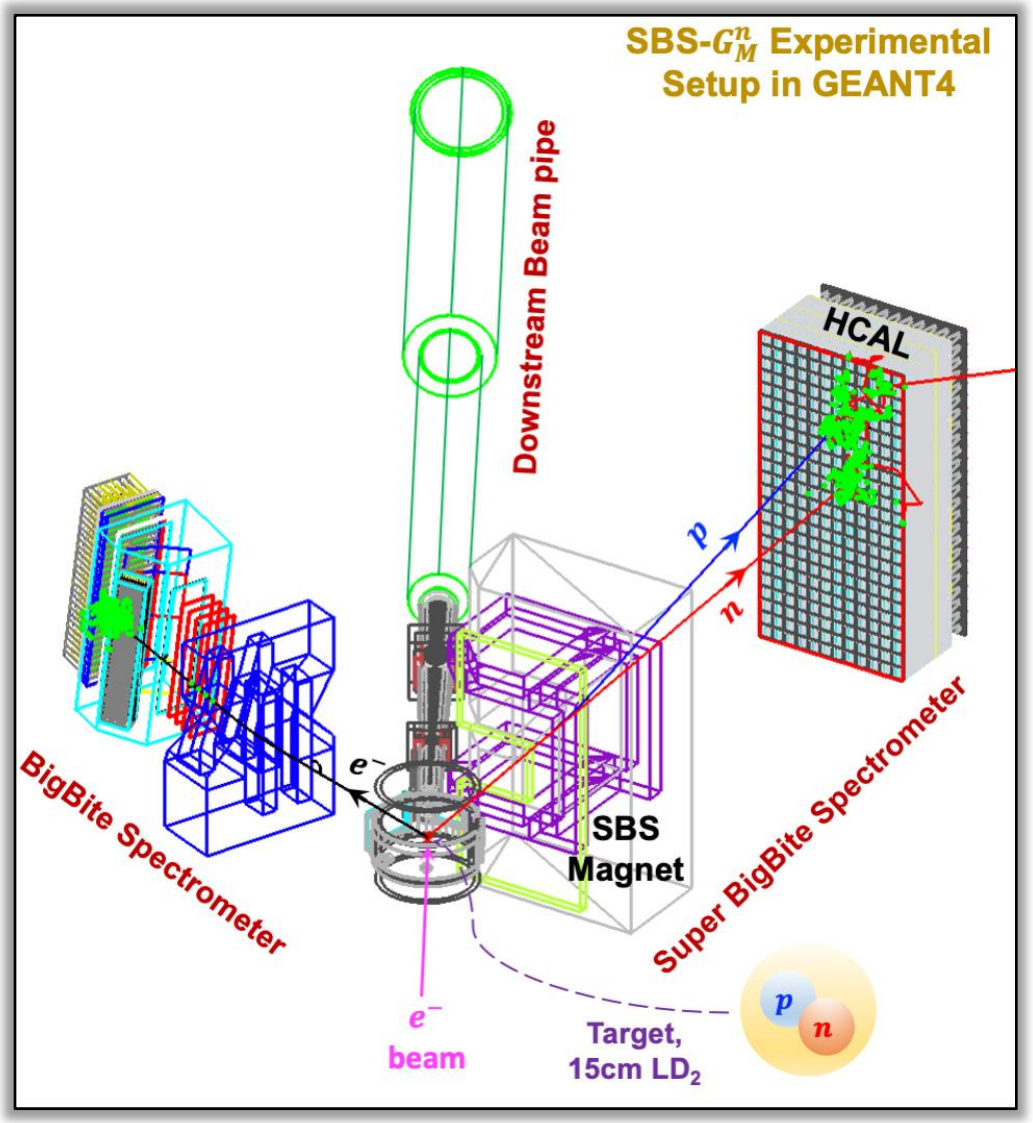

Physics Analysis Methods – Introducing HCAL Δx Variable

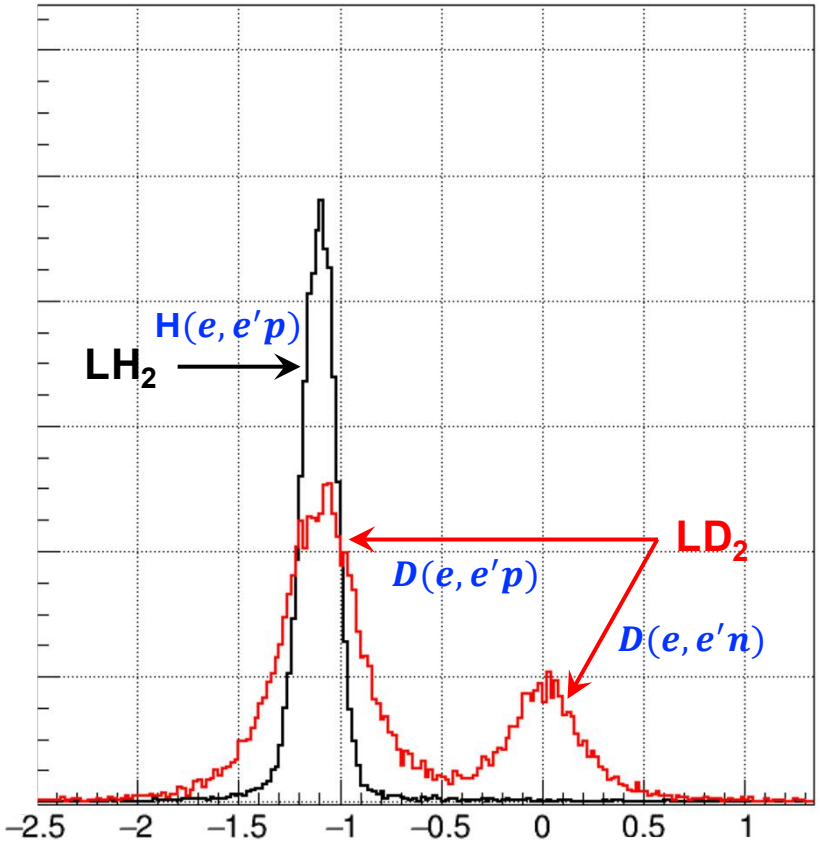

$\Delta x = x_{HCAL}^{meas} - x_{HCAL}^{pred}$ (m)

x_{HCAL}^{meas} ⇒ Measured Proton/Neutron Position at HCAL
x_{HCAL}^{pred} ⇒ Predicted **Neutron** Position at HCAL

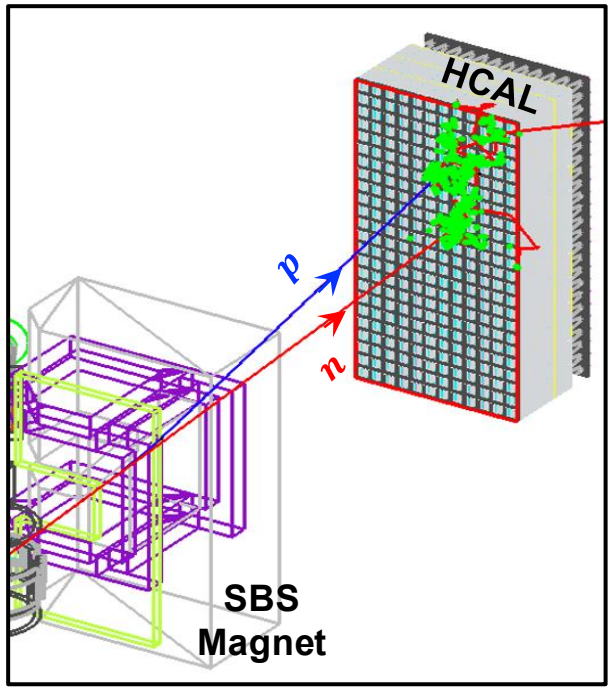

- From the Δx plot we can extract $D(e,e'n)$ & $D(e,e'p)$ counts to form ratio of interest:

$$R^{QE} = \frac{\frac{d\sigma}{d\Omega}\Big|_{D(e,e'n)}}{\frac{d\sigma}{d\Omega}\Big|_{D(e,e'p)}}$$

Analysis Cuts

- **Good *e* Track Selection Cuts:**
  - Track quality
  - Pion rejection
- **Good HCAL Event Selection:**
  - HCAL cluster energy
  - HCAL active area
- **Good Coincidence Event Selection:**
  - Shower-HCAL ADC coincidence time
- **Quasi-Elastic Event Selection Cuts:**
  - W^2
  - Δy
- **Fiducial Cut**
  - to match acceptance for proton and neutron events

Effect of Fiducial Cut: $Q^2 = 3\ (GeV/c)^2$

No Fiducial Cut

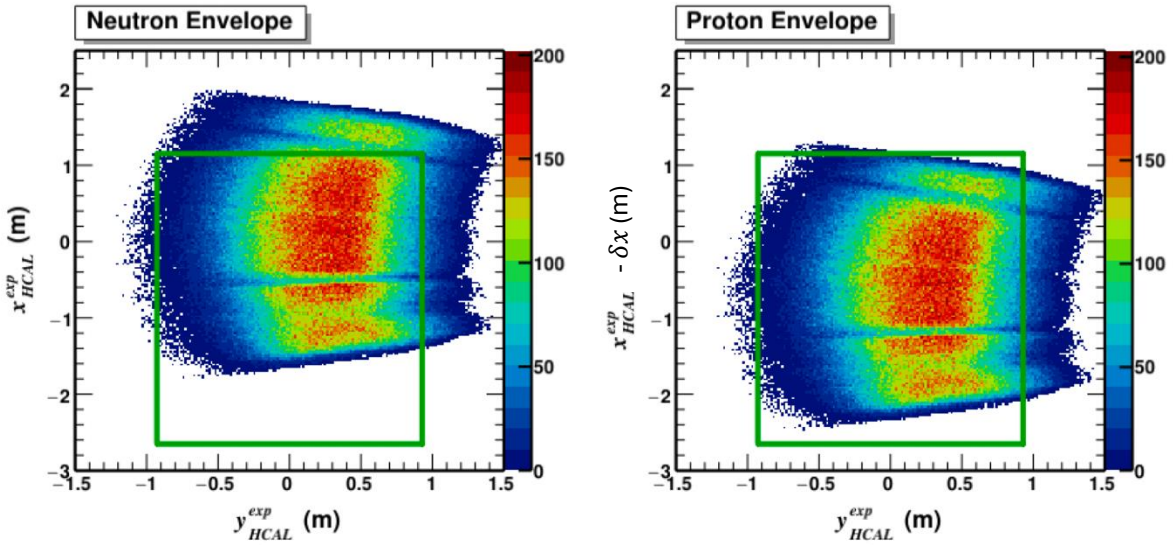

--- Top of HCAL ---

With Fiducial Cut

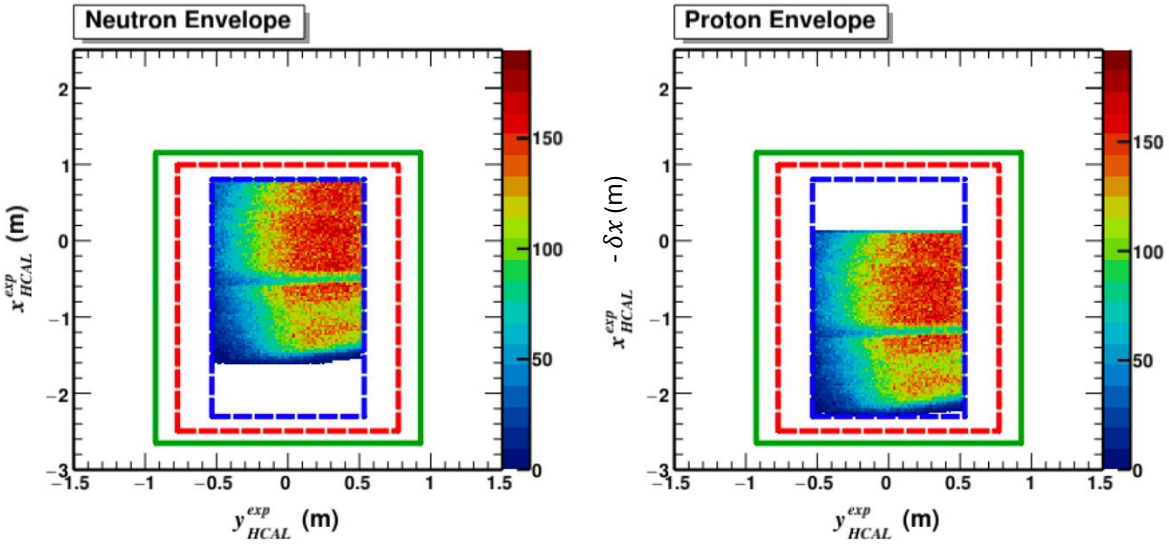

--- Top of HCAL ---

HCAL Physical Boundary

HCAL Active Area

HCAL Safety Margin

- Fiducial cut effectively matches the acceptances for D(e,e'n) and D(e,e'p) events, essential to reduce systematic error in the ratio.

Effect of Analysis Cuts: $Q^2 = 3\ (GeV/c)^2$

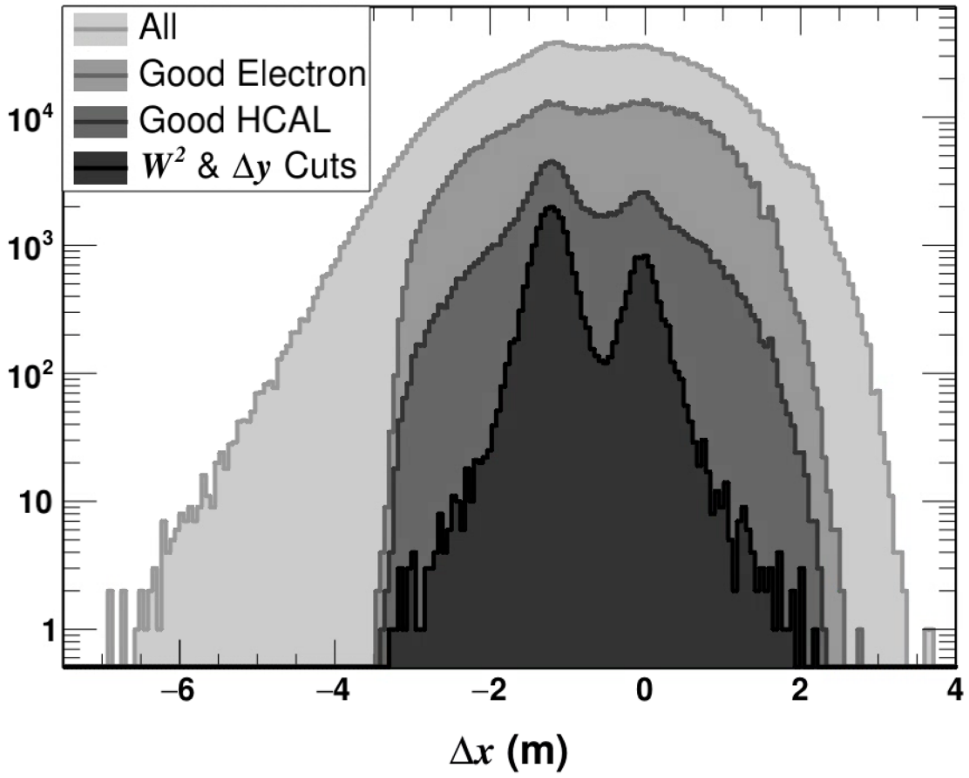

Quasi-Elastic (QE) Event Selection: $Q^2 = 3\ (GeV/c)^2$

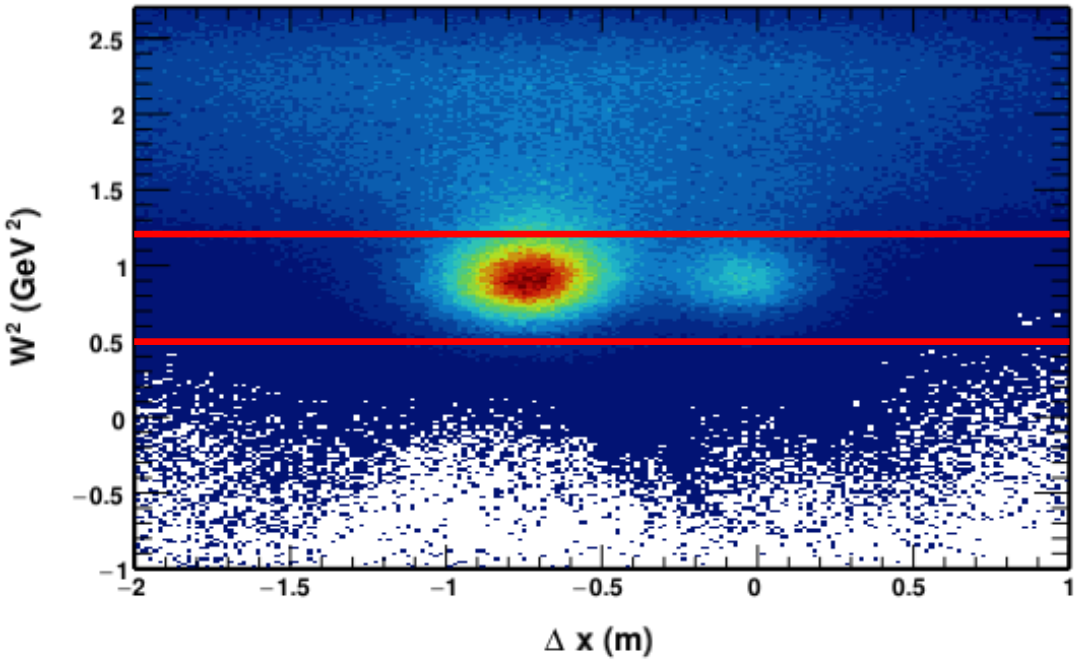

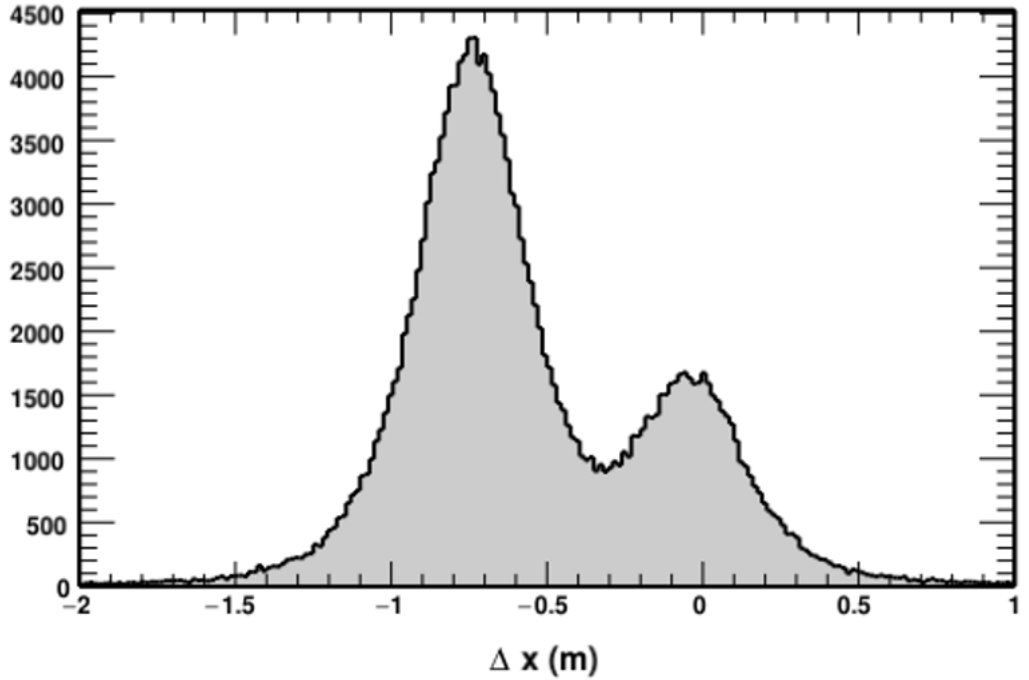

- Squared invariant mass of the virtual photon–struck nucleon system:

$$W^2 = (P_N^i + q)^2$$
$$= M_N^2 \quad \text{(Elastic Scattering)}$$

Quasi-Elastic (QE) Event Selection Across Q^2 Points

Q^2 = 3 (GeV/c)^2

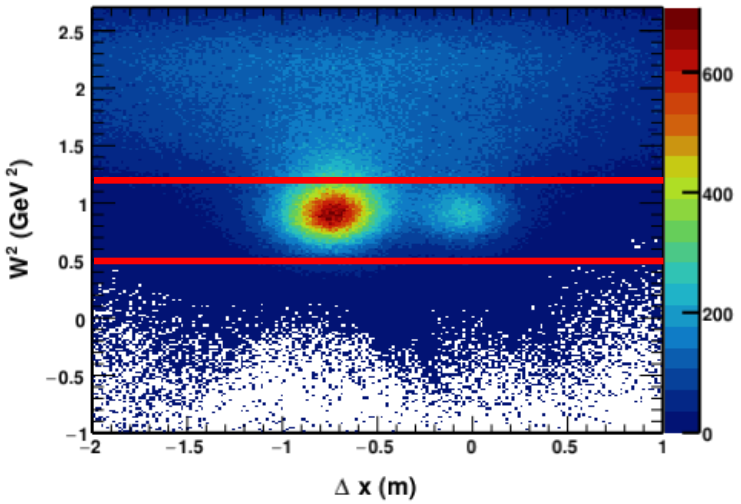

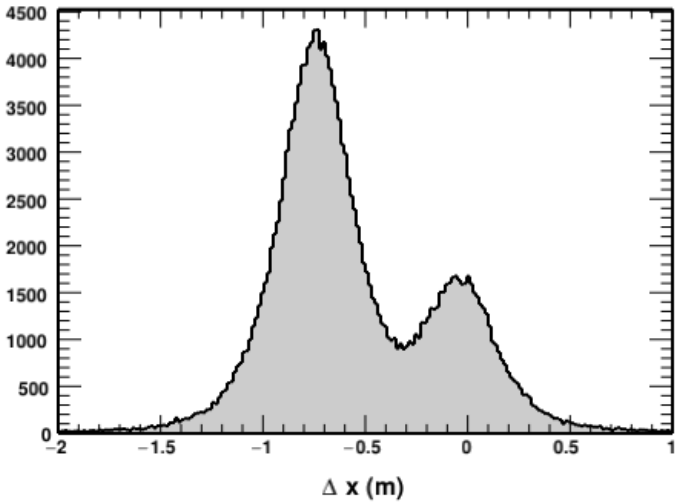

Q^2 = 7.4 (GeV/c)^2

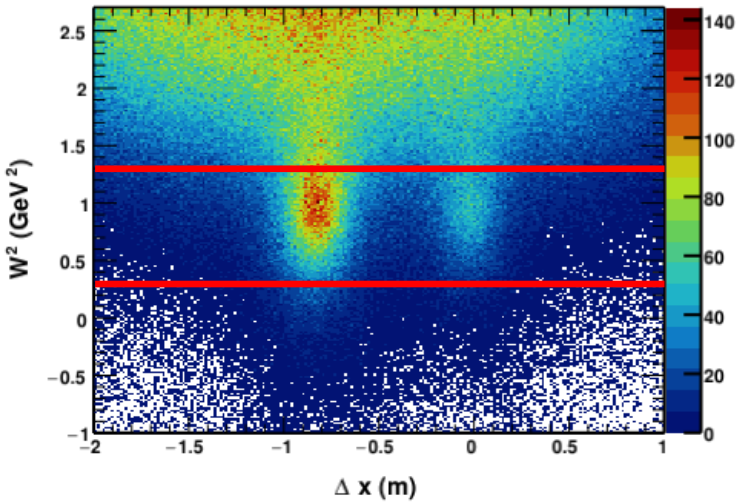

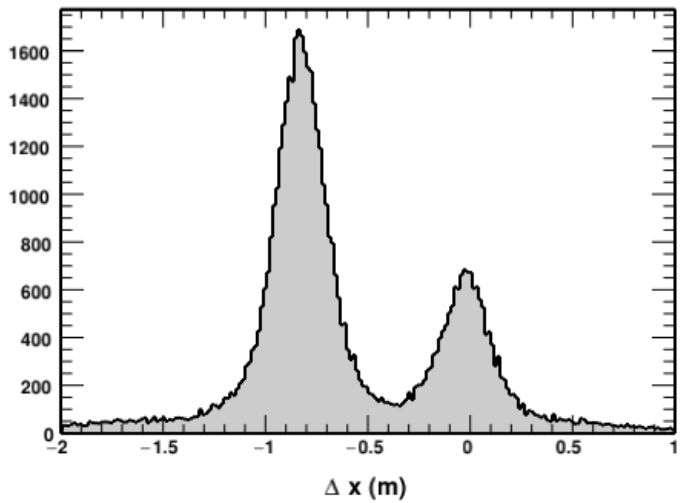

Q^2 = 13.5 (GeV/c)^2

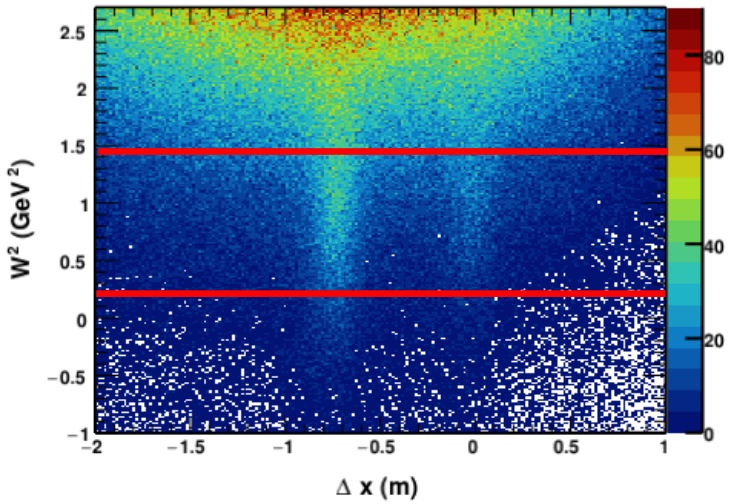

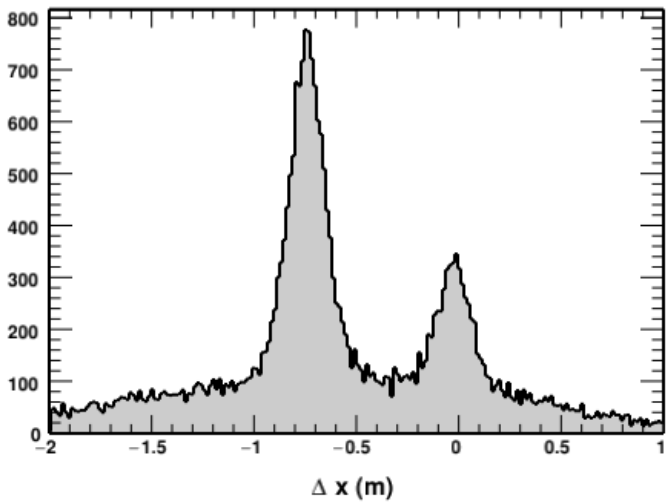

Signal Shapes from Monte Carlo (MC) Simulation

❖ Steps to generate realistic signal shapes from MC:

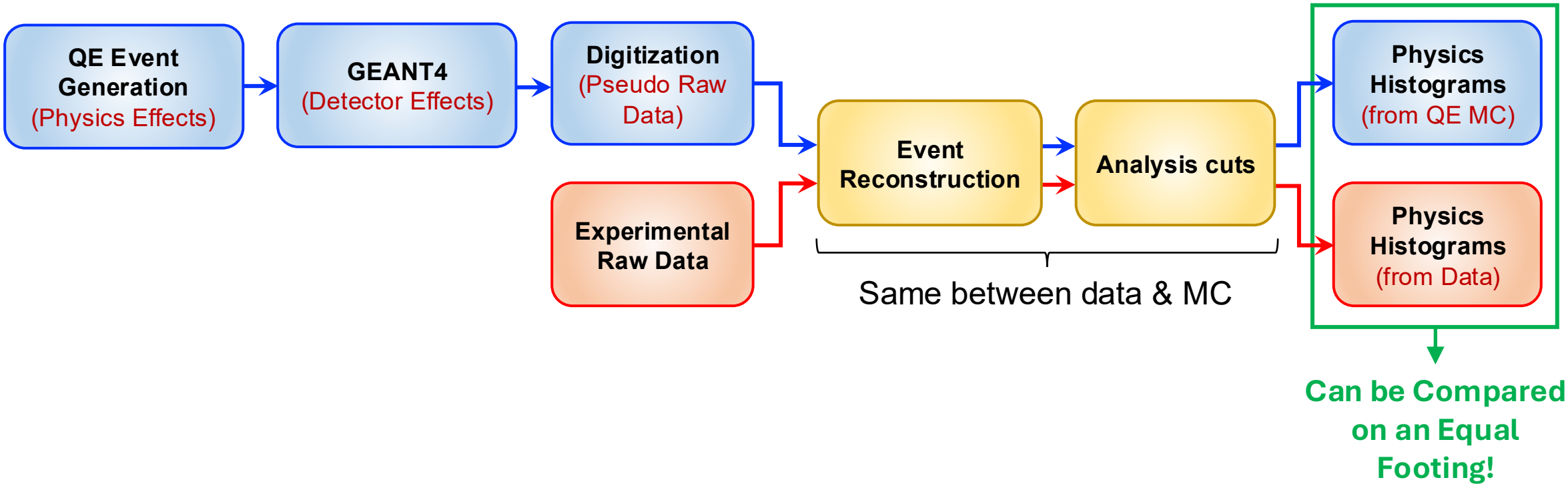

W^2 Distribution from Quasi-Elastic MC

Generated using Quasi-Elastic MC

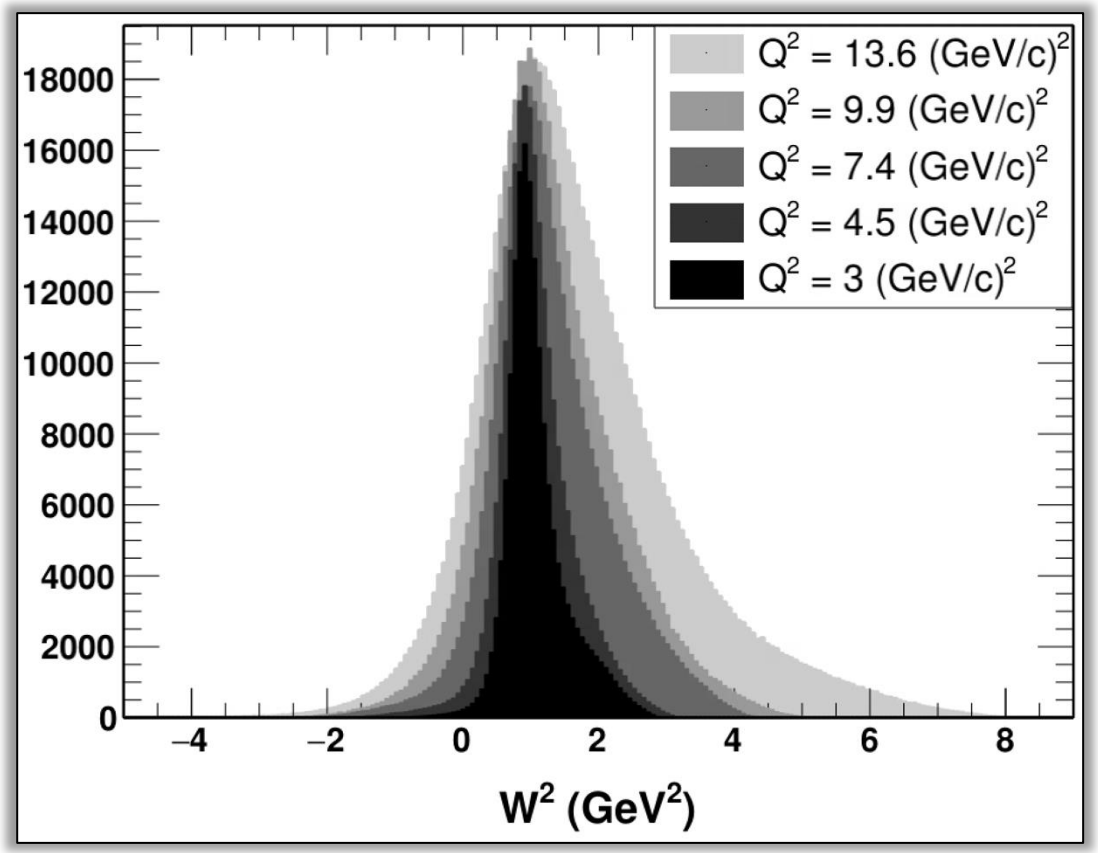

❖ The kinematic broadening of the W^2 distribution with increasing Q^2 is accurately produced in the MC.

Qualitative Data/MC Comparison of the W^2 Distribution

Data/MC Comparison for Q^2 = 13.5 (GeV/c)^2

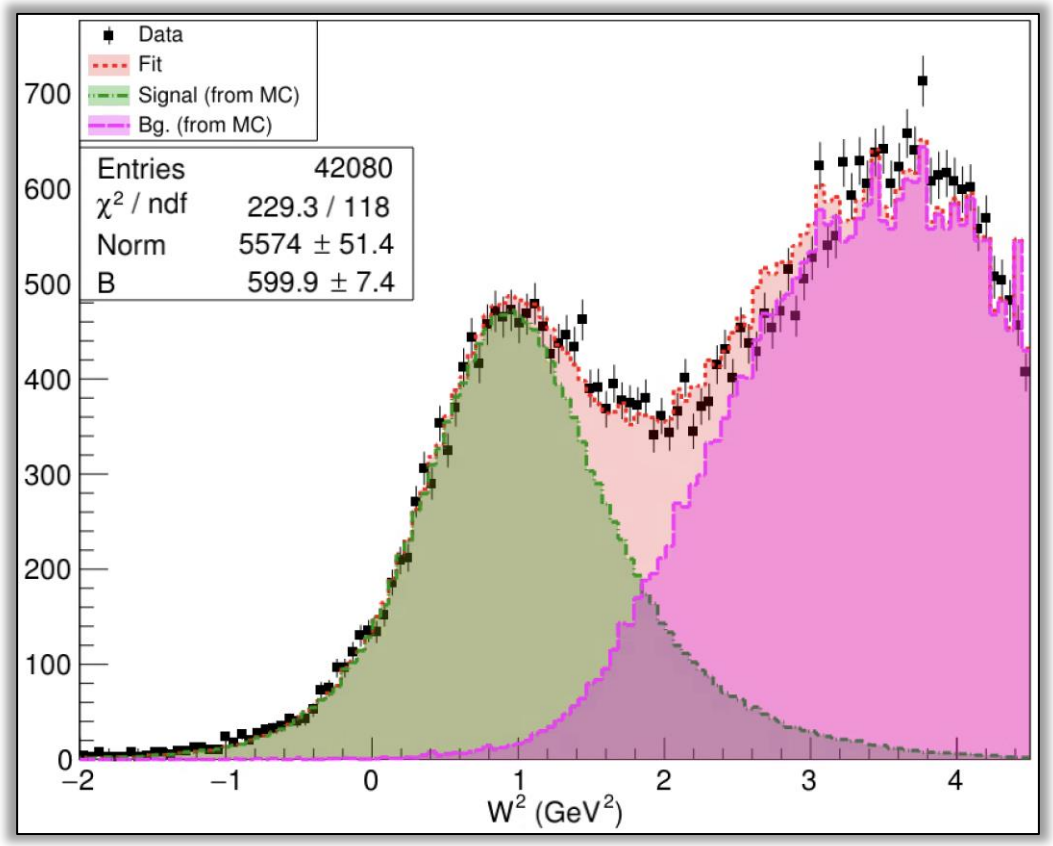

❖ Qualitative data/MC comparison looks encouraging even for the most challenging kinematics.

Data/MC Fit to Δx Distribution: $Q^2 = 7.4\ (\mathrm{GeV/c})^2$

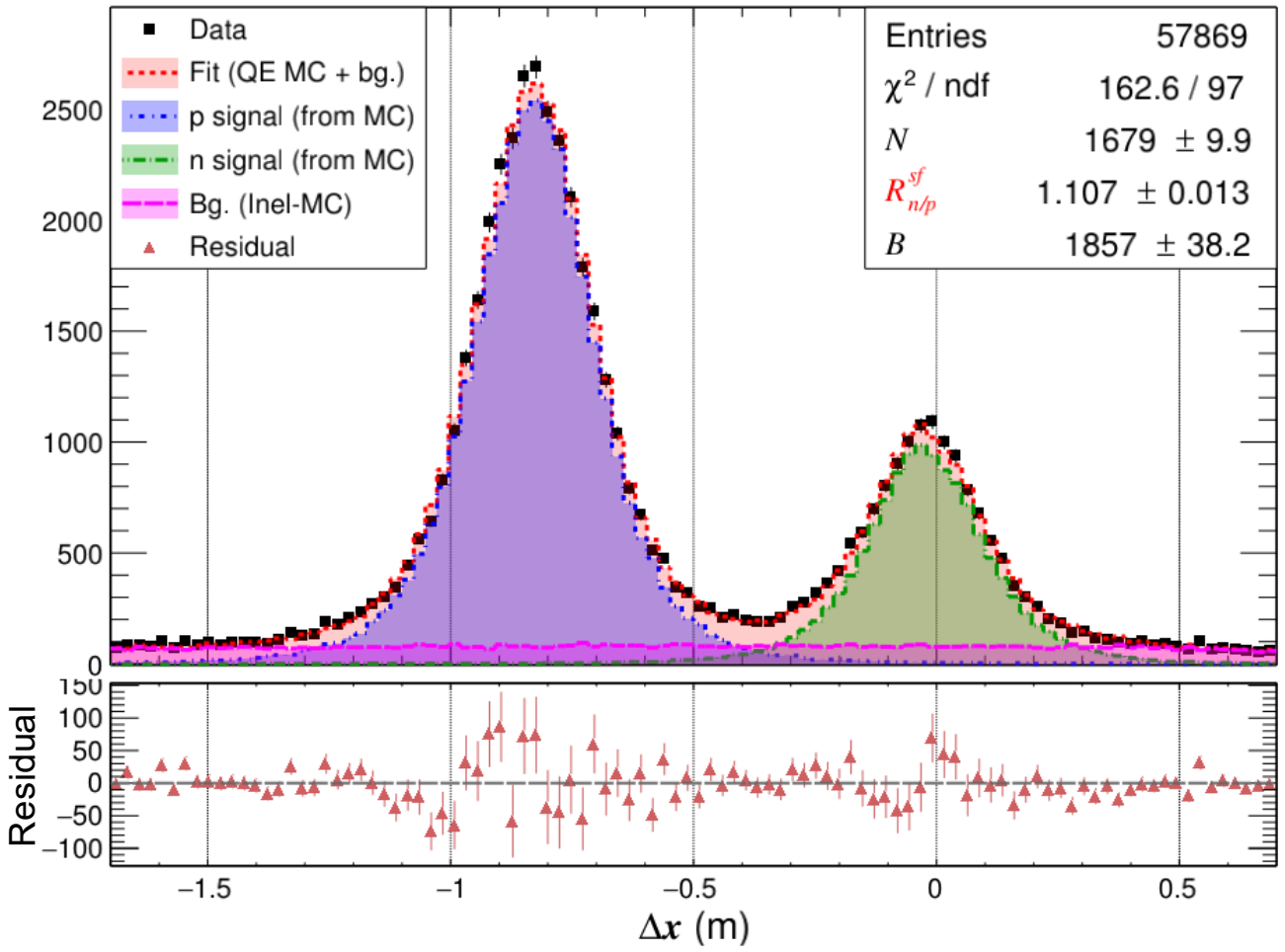

- Fit equation:

$$\mathrm{Data} = N * (\mathrm{p}^{\mathrm{MC}}_{\mathrm{signal}} + R^{sf}_{n/p} * \mathrm{n}^{\mathrm{MC}}_{\mathrm{signal}}) + B * \mathrm{Inel}^{\mathrm{MC}}_{\mathrm{bg}}$$

- Fit parameters:
  1. N – Overall proton (p) normalization.
  2. $R^{sf}_{n/p}$ – Relative neutron (n) to proton normalization.
  3. B – Overall background normalization.

- Agreement of fit looks good in the entire range of interest.

GMn Extraction from Data/MC Fit : $Q^2 = 7.4\ (GeV/c)^2$

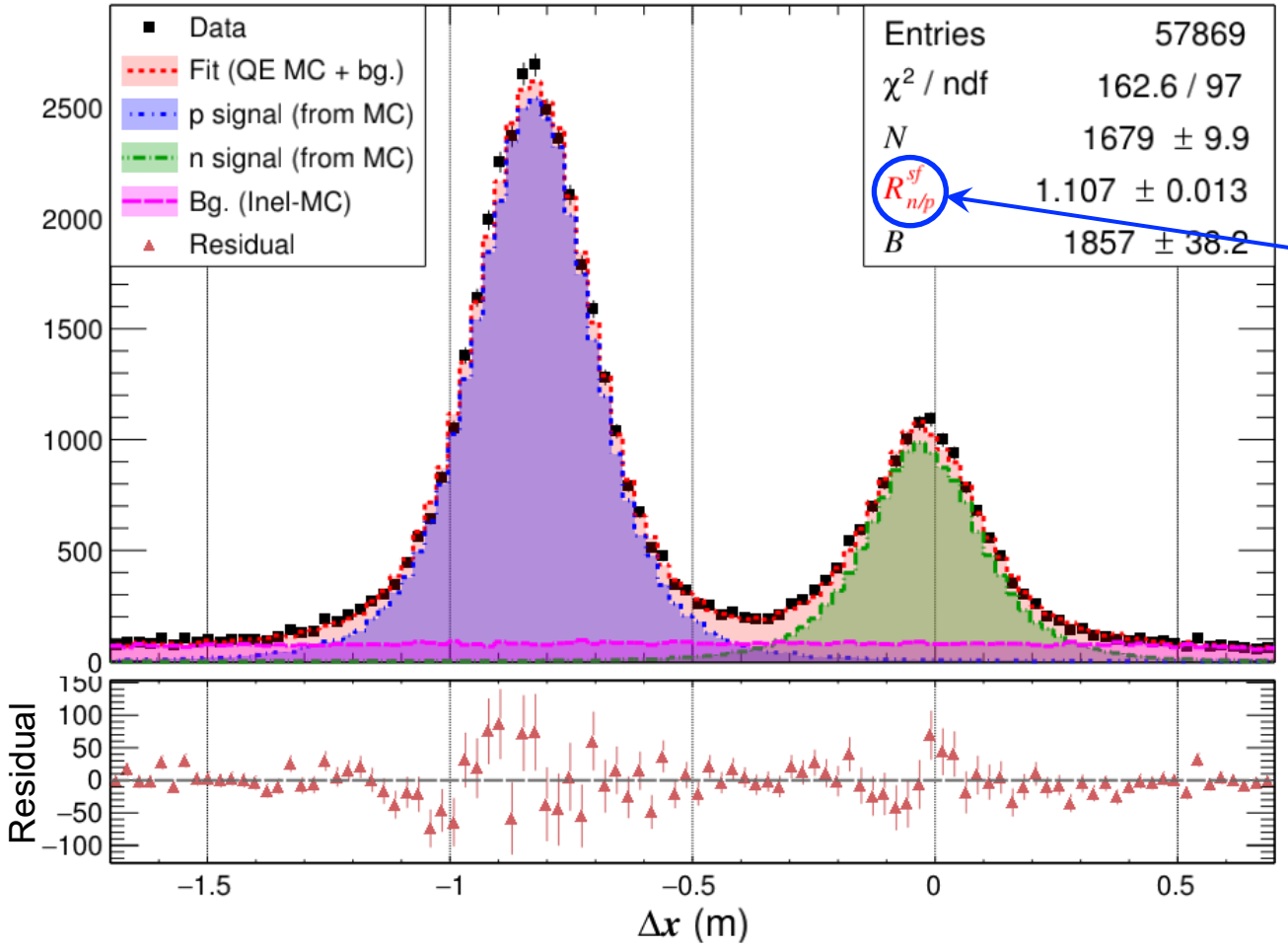

- Assumption:
  - Simulation accurately represents nuclear, radiative, and detector effects that are known to be present in data.
- Interpretation:
  - The fit parameter $R^{sf}_{n/p}$, i.e. the relative n/p normalization, is a measure of the discrepancy in the neutron to proton Born cross section ratio between simulation and data.
- GMn extraction:

$$R = \frac{\frac{d\sigma}{d\Omega}\Big|_{n(e,e')}}{\frac{d\sigma}{d\Omega}\Big|_{p(e,e')}} = R^{sf}_{n/p} * R_{MC}$$

$$\Rightarrow G^n_M = -\left[\frac{1}{\tau_n}\frac{\epsilon_n(1+\tau_n)}{\epsilon_p(1+\tau_p)}\sigma^p_{Red}R - \frac{\epsilon_n}{\tau_n}G^{n\,2}_E\right]^{\frac{1}{2}}$$

Total Systematic Error Budget (Preliminary)

Table 2: Estimated contributions (in percent) to systematic error on R and $\frac{G_M^n}{\mu_n G_D}$.

	Error Sources	Q^2 (ϵ)				
		3 (0.72)	4.5 (0.51)	7.4 (0.46)	9.9 (0.50)	13.5 (0.41)
$\Delta(R)_{sys}$	Inelastic Cont.	0.33	0.75	0.84	0.75	2.67
	Nucleon Det. Effi.	2.00	2.01	2.01	2.02	2.02
	Radiative Corr.	2.31	3.32	3.77	3.87	5.47
	Cut Stability	0.16	0.15	0.40	0.67	0.60
	FSI	0.04	0.01	0.02	0.02	0.03
	Total	3.08	3.95	4.37	4.48	6.44
$\Delta(\frac{G_M^n}{\mu_n G_D})_{sys}$	Inelastic Cont.	0.17	0.38	0.42	0.37	1.34
	Nucleon Det. Effi.	1.00	1.00	1.01	1.01	1.01
	Radiative Corr.	1.16	1.66	1.88	1.94	2.73
	Cut Stability	0.03	0.07	0.20	0.33	0.30
	FSI	0.02	0.00	0.01	0.01	0.01
	σ_{Red}^p	0.82	0.92	1.35	1.52	1.33
	G_E^n	0.55	0.65	0.62	0.66	0.55
	Total	1.83	2.27	2.64	2.79	3.53

Preliminary Results

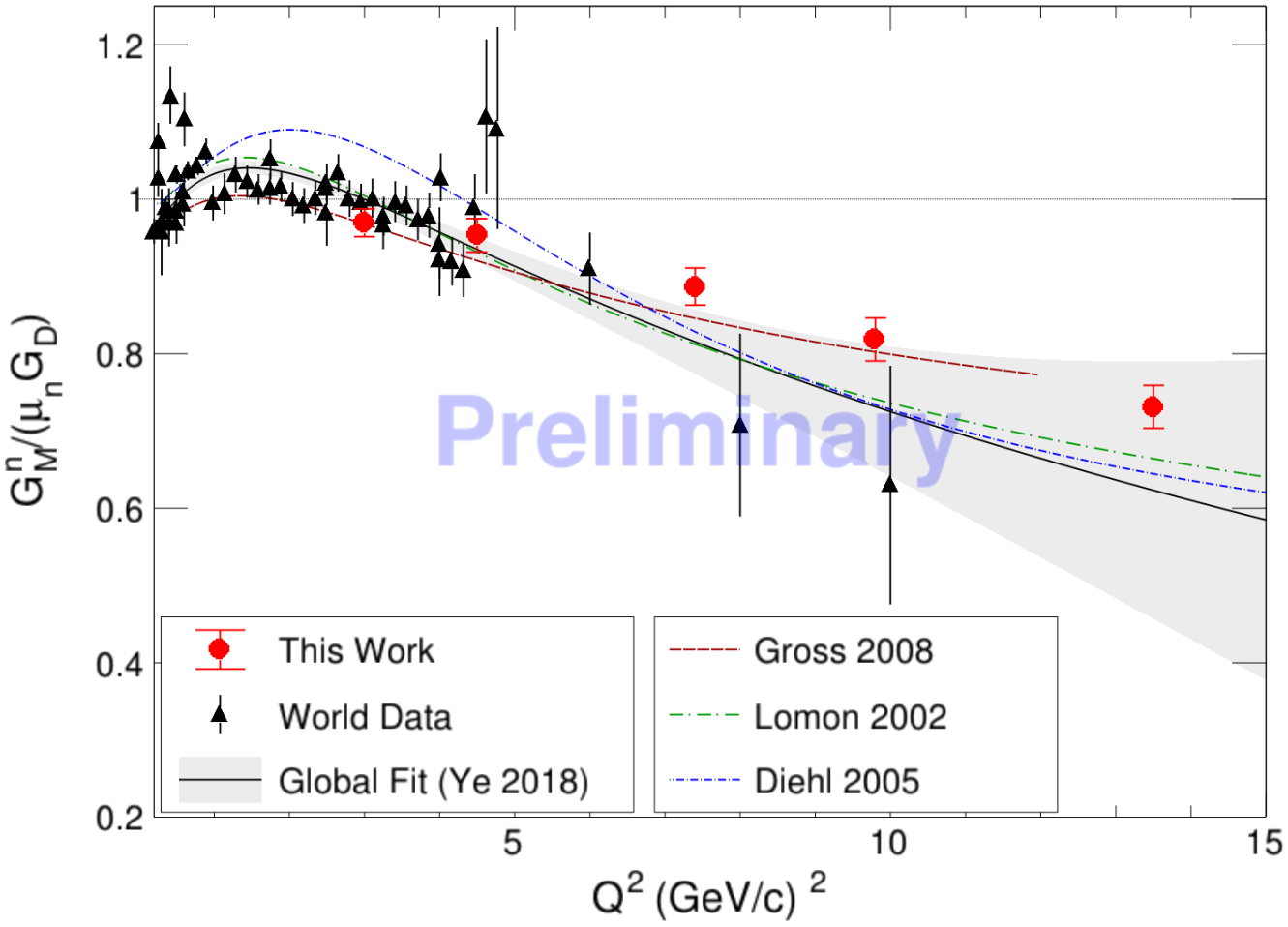

- High-precision GMn now extends to Q^2 = 13.5 GeV^2—more than doubling the previous reach.
- The 13.5 GeV^2 point delivers ~2 times better precision than the earlier 6 GeV^2 result and is likely to remain unmatched for years.
- Results are consistent with the global trend; the updated fit in progress will tightly constrain the high-Q^2 region providing much greater discrimination power between different models.
- Improved flavor-decomposed form factors and nucleon transverse density extractions.

- Statistical and Systematic errors have been added in quadrature.

Impact on the Quark Form Factors (Preliminary)

- Flavor Decomposition of Magnetic Form Factors:

$$G_M^u = 2G_M^p + G_M^n$$
$$G_M^d = 2G_M^n + G_M^p$$

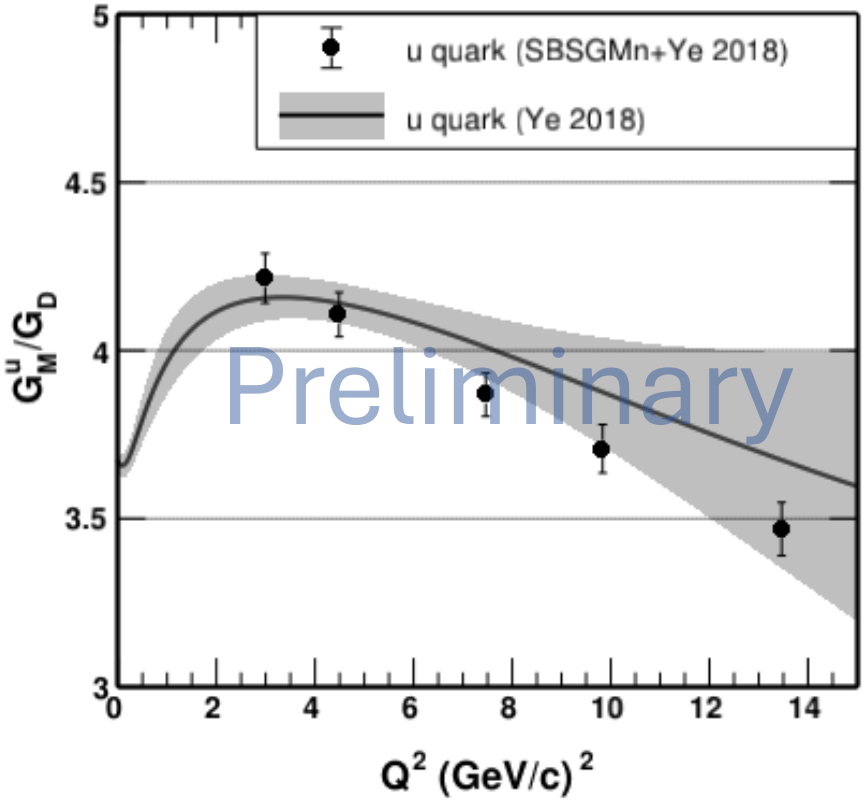

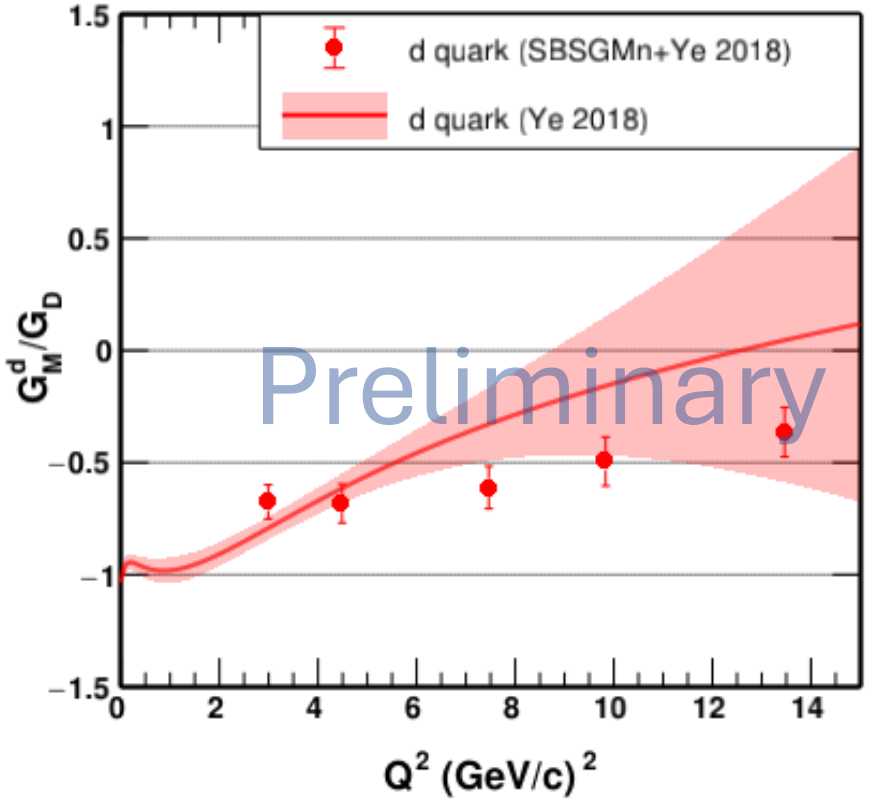

- The bands represent flavor decomposition from Ye 2018 fit.
- The points are obtained by replacing G_M^n values from the fit with the ones from this work.

Impact on the Quark Form Factors (Preliminary) contd.

- Flavor Decomposition of Dirac Form Factors:

$$F_1^u = 2F_1^p + F_1^n$$
$$F_1^d = 2F_1^n + F_1^p$$

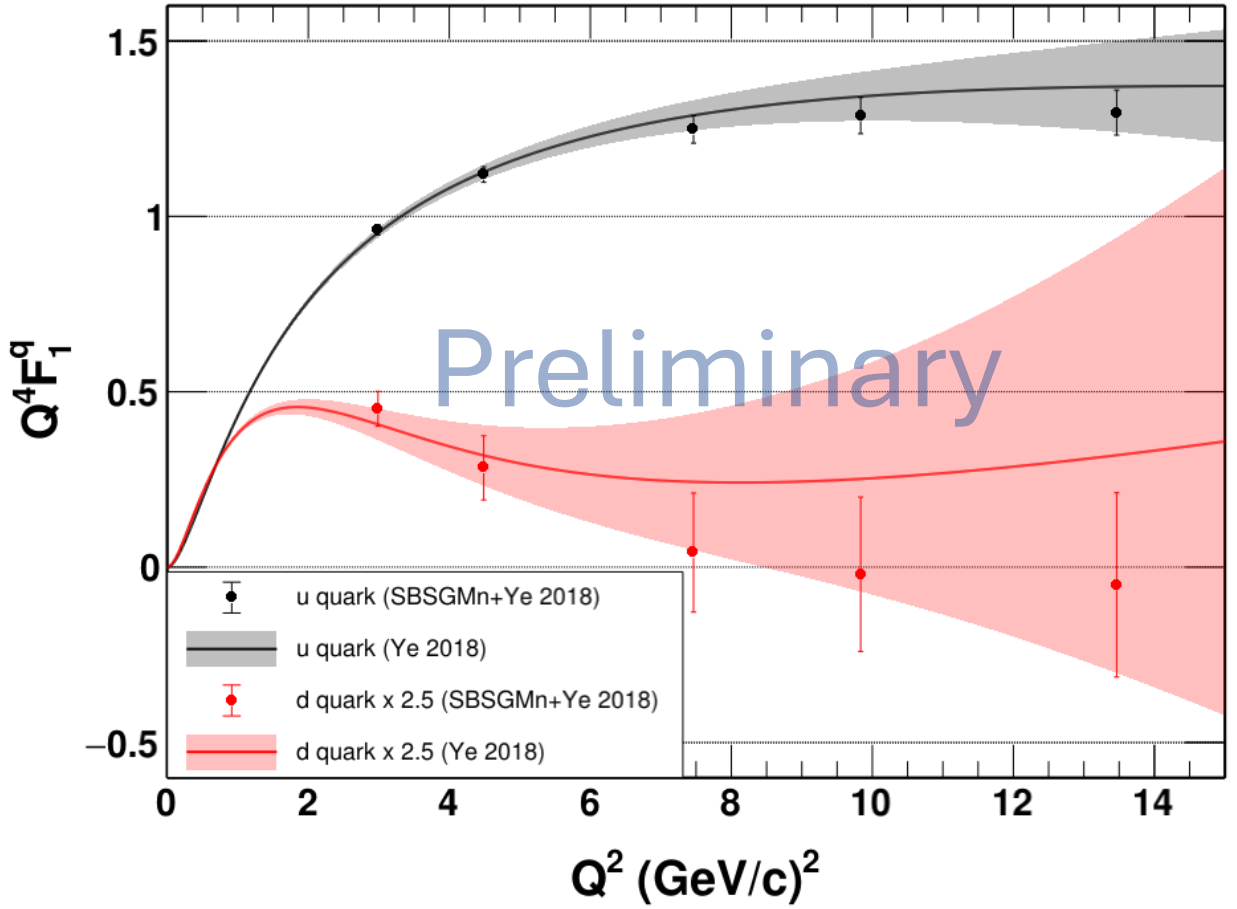

- Possible zero-crossing of $\boldsymbol{F_1^d}$ at $\mathbf{Q^2 = 9.8 \pm 1.8\ (GeV/c)^2}$ (obtained from a linear fit to data).
- Uncertainty is dominated by G_E^n. SBS-GEn will improve the situation significantly!

Outline

- Nucleon Form Factors and the Structure of the Nucleon
- A Brief Overview of the SBS-GMn Experiment
- Physics Analysis Methodology, Challenges, and Preliminary Results
- Status of 3rd Reconstruction Pass – The Last Step to Finalize Results
- Summary and outlook

3rd Pass of Reconstruction – Necessity and Improvements

HCal-Shower Coincidence Time from
2nd Reconstruction Pass

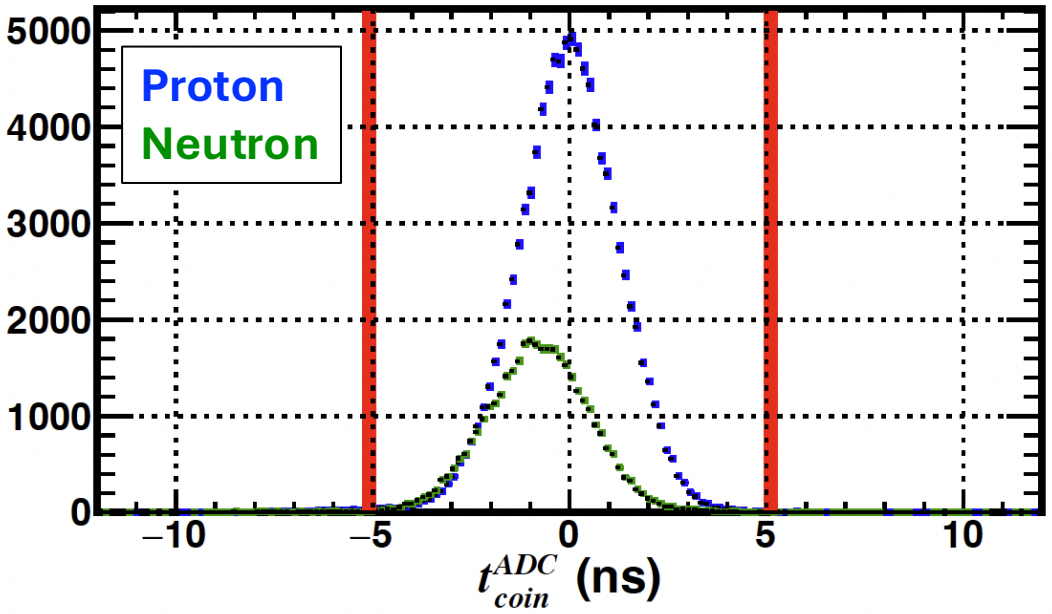

Position-dependent non-uniformity in the HCal timing calibration, lingering after the 2nd reconstruction pass, affected *D(e,e'p)* and *D(e,e'n)* events differently, biasing the ratio of interest. This necessitated a 3rd pass of calibration and reconstruction of the entire dataset which completed a couple of weeks ago.

Improvements achieved in 3rd Pass:

Greatly improved timing hodoscope calibration achieved via a simultaneous fit of various correction factors (RF, e-ToF, time-walk, propagation delay, cable length, etc.), as proposed and implemented by Andrew Puckett.

Implementation of right prescription to compare TDC and ADC times enabling the alignment of BBCal and HCal time with respect to the calibrated timing hodoscope.

Implementation of nucleon ToF correction to HCal time.

3rd Pass of Reconstruction – Results

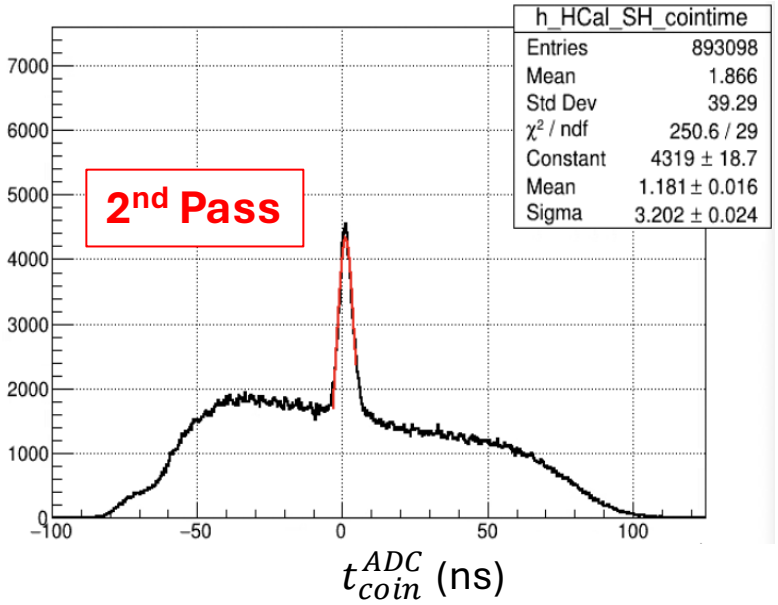

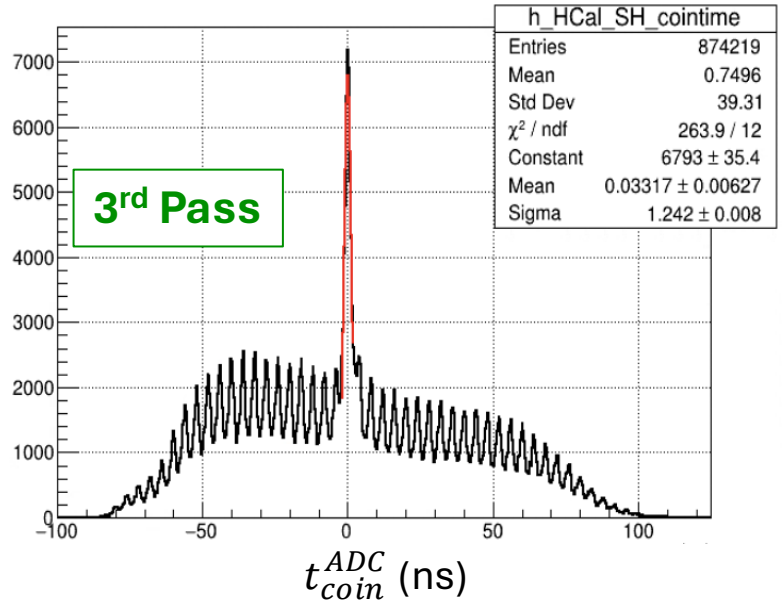

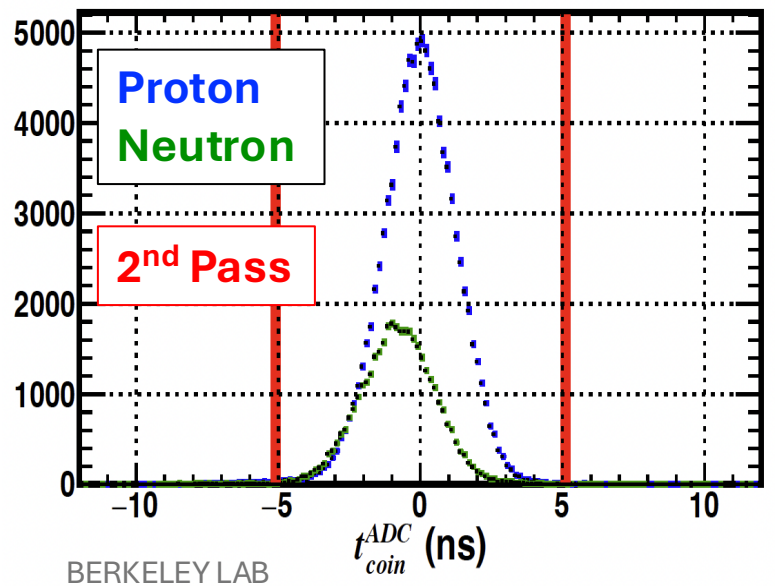

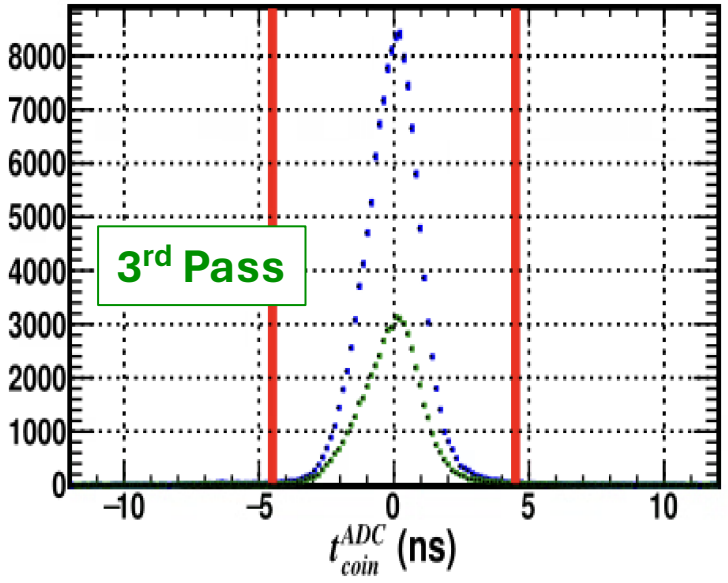

Greatly improved HCal-Shower ADC coincidence time resolution good enough to resolve the beam bunch structure.

Mitigation of position-dependent non-uniformity in HCal timing calibration better aligns the coincidence times for *D(e,e'p)* and *D(e,e'n)* events.

Summary and Outlook

- SBS-GMn, the first SBS experiment, ran from fall 2021 to Feb 2022, to extend the range of high-precision G_M^n measurement from $Q^2 = 6$ to $13.5\ (\mathrm{GeV/c})^2$.
- The extracted preliminary results are in line with our precision goals and will vastly advance the current understanding of the neutron's internal structure.
- A third pass of calibration and reconstruction successfully addressed lingering HCal timing issues, allowing for the finalization of analysis.
- Significant efforts are ongoing to publish these beautiful results as soon as possible. Stay tuned!

Acknowledgements

- Thanks to SBS-GMn and -nTPE Graduate Students – Vanessa Brio (Catania U.), John Boyd (UVA), Provakar Datta (UConn), Nathaniel Lashley-Colthirst (Hampton U.), Ralph Marinaro (University of Glasgow), Anuruddha Rathnayake (UVA) , Maria Satnik (W&M), Sebastian Seeds (UConn), Ezekiel Wertz (W&M)
- Thanks to SBS-GMn Spokespeople – Bogdan Wojtsekhowski (JLab), Brian Quinn (CMU), Alexandre Camsonne (JLab)
- Special thanks to Andrew Puckett (UConn) for his unparallel contribution to SBS software and analysis.
- Thanks to the Jefferson Lab Hall A collaboration and of course the SBS collaboration and anyone else who has contributed to the success of SBS-GMn.
- Thanks to US Department of Energy Office of Science, Office of Nuclear Physics, for supporting this work.

Thank You for Your Attention!

Questions? Comments?

Backup Slides

Quark Flavor Decomposition of Nucleon Form Factors

Scaling goes like $1/Q^2$. Indicates 1 gluon exchange i.e., scattering from the lone "outside" u quark.

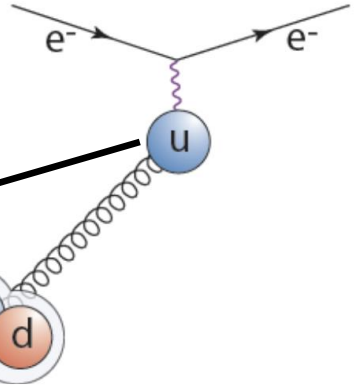

- Assumption of charge symmetry enables us to perform a quark flavor decomposition of the nucleon form factors, $F_1^{p(n)}$ and $F_2^{p(n)}$, in the form:

$$F_{1(2)}^{u} = 2F_{1(2)}^{p} + F_{1(2)}^{n}$$
$$F_{1(2)}^{d} = 2F_{1(2)}^{n} + F_{1(2)}^{p}$$

Ref: Cates *et al*: Phys. Rev. Lett. 106, 252003 (2011)

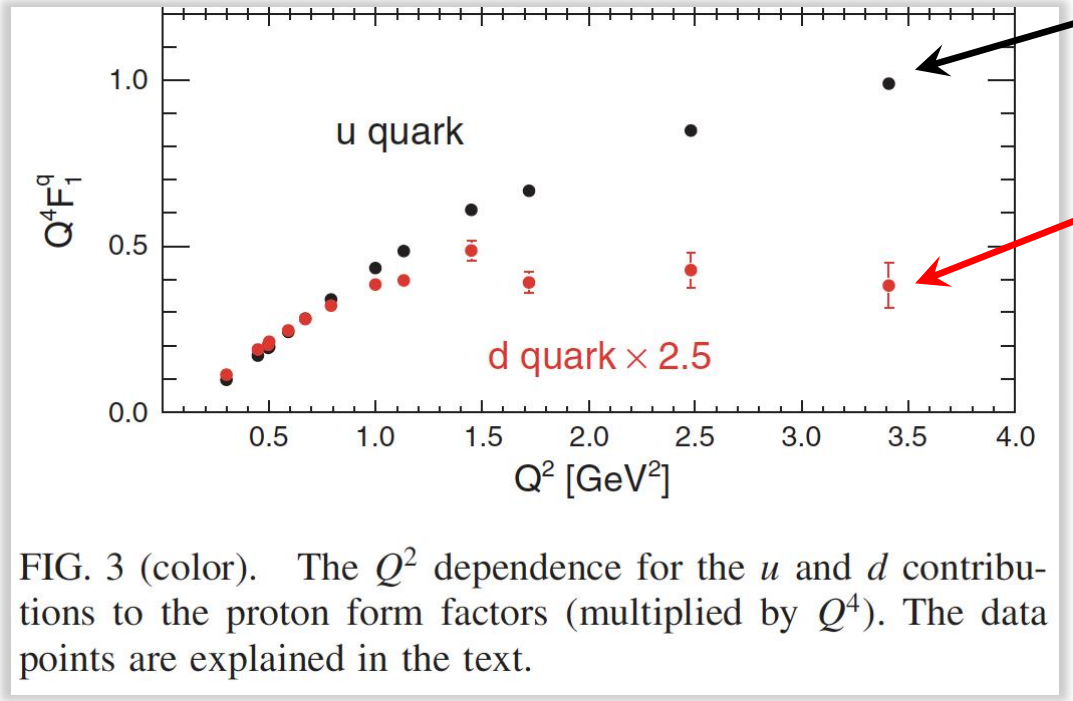

FIG. 3 (color). The Q^2 dependence for the u and d contributions to the proton form factors (multiplied by Q^4). The data points are explained in the text.

Scaling goes like $1/Q^4$. Indicates 2 gluons exchange i.e., probing inside the diquark.

- u and d quark FFs show dramatically different Q^2 dependence!
- Naïve scaling argument proposed by Gerry Miller invokes diquark degrees of freedom.

Far-Reaching Significance of Form Factor Measurements

- By assuming charge symmetry, flavor decomposition of the nucleon form factors is possible. The u and d quark form factors show dramatically different Q^2 dependence. A possible explanation invokes diquark degrees of freedom within the nucleons.

$$F^u_{1(2)} = 2F^p_{1(2)} + F^n_{1(2)} \qquad F^d_{1(2)} = 2F^n_{1(2)} + F^p_{1(2)}$$

- Nucleon form factors constraint GPDs through sum rules and enable their extraction from hard exclusive processes.

$$F_1^q(t) = \int_0^1 \mathrm{d}x H_v^q(x,t) \qquad F_2^q(t) = \int_0^1 \mathrm{d}x E_v^q(x,t)$$

The CEBAF at Jefferson Lab (JLab)

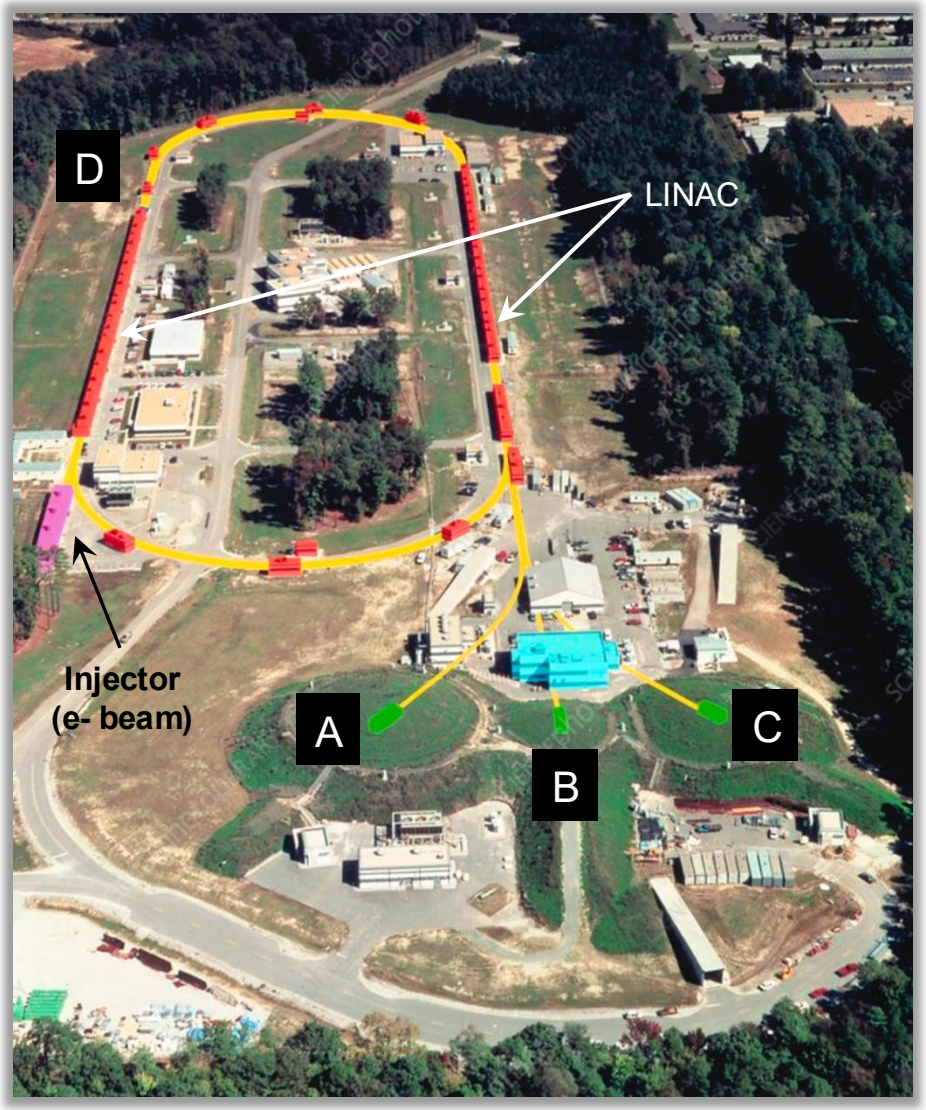

CEBAF at Jefferson Lab (JLab) [Aerial View]

- Jefferson Lab (JLab) is a DoE owned national accelerator facility located in Newport News, VA.
- The Continuous Electron Beam Accelerator Facility (CEBAF) at Jefferson Lab is a racetrack-shaped electron accelerator located 25 feet underground.
- It can deliver up to 12 GeV continuous wave (CW) electron beam with unparalleled intensity and precision.
- JLab has 4 experimental Halls – A, B, C, & D. SBS-GMn ran in Hall A.

BigBite Calorimeter (BBCAL): Pre-Shower

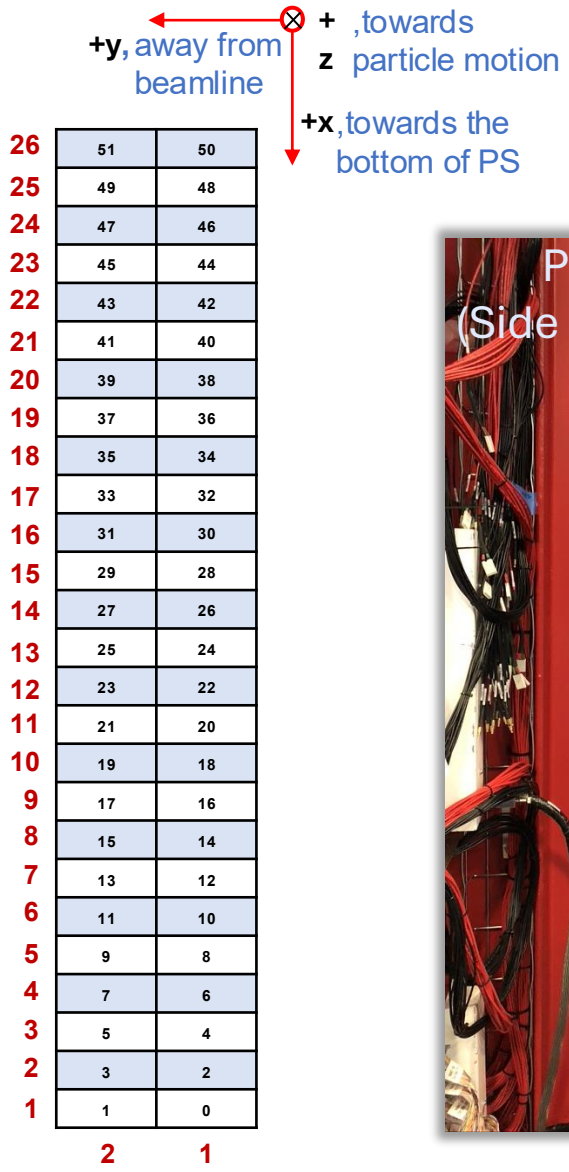

- PS is made of 52 rad-hard lead-glass blocks.
- Signals generated in each block are readout by a PMT.
- Block dimension: 9 x 9 x 29.5 cm^3
- Blocks are stacked in 26 rows of 2 columns facing each other.
- mu-metal shielding around each block.

BigBite Calorimeter (BBCAL): Shower

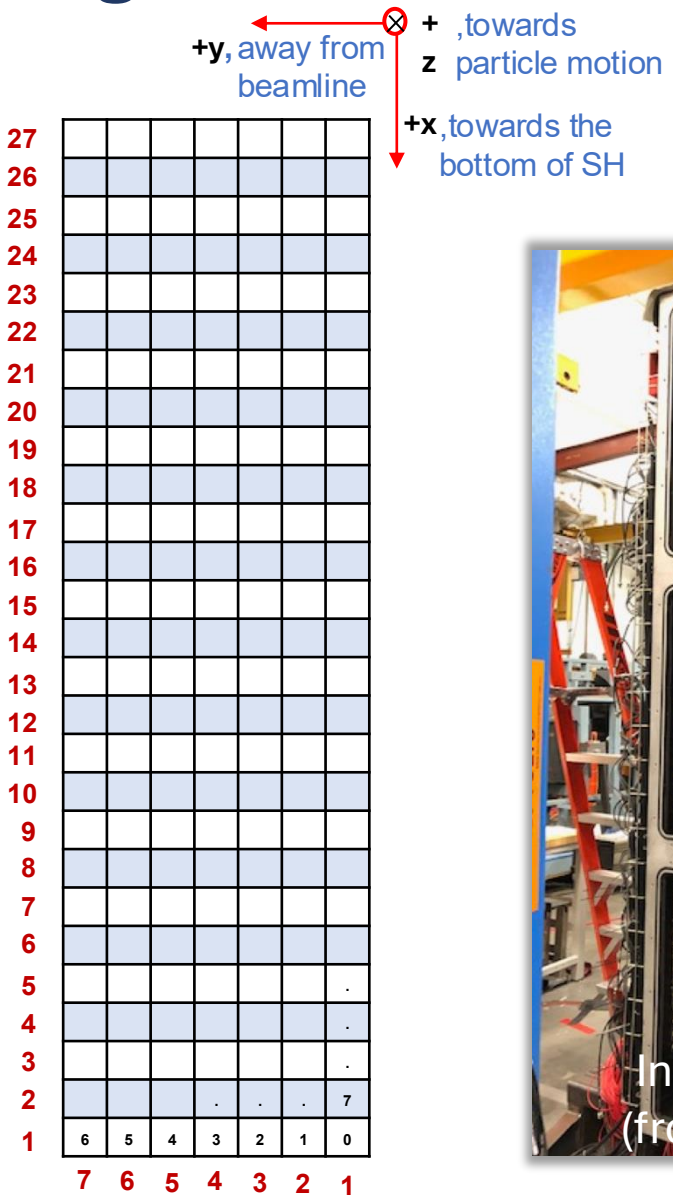

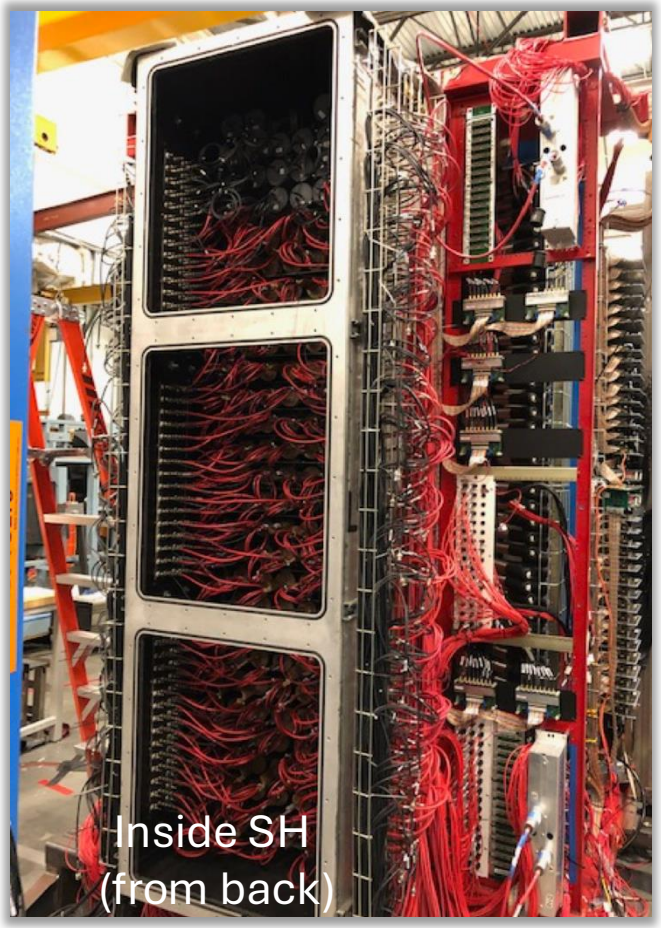

- BB Shower is made of 189 lead-glass blocks.
- Signals generated in each block are readout by a PMT.
- Block dimension: 8.5 x 8.5 x 34 cm^3
- Blocks are stacked in 27 rows of 7 columns facing the spectrometer axis.
- mu-metal shielding outside & between rows.

Hadron Calorimeter (HCAL)

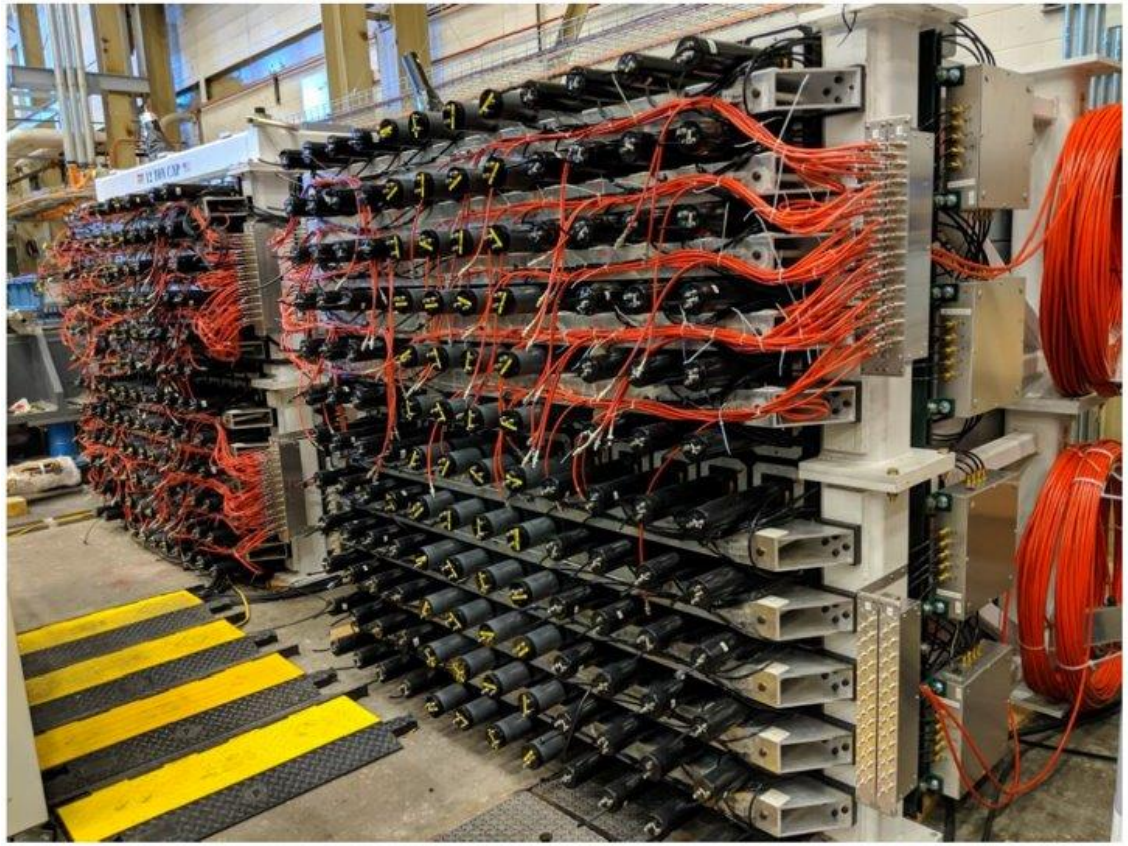

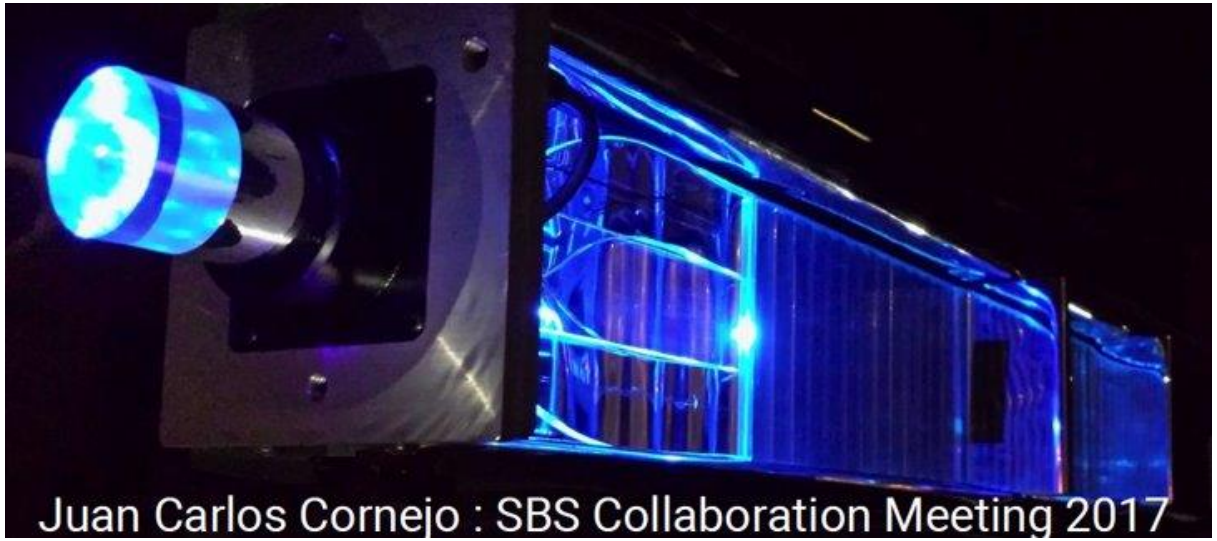

Kinematics of SBS-GMn (Detailed)

Table I: Kinematics of SBS-GMn. Q^2 is the central Q^2, E_{beam} is the beam energy, $\theta_{BB}(d_{BB})$ is the BigBite central angle (target-magnet distance), $\theta_{SBS}(d_{SBS})$ is the Super BigBite central angle (target-magnet distance), $\theta_{HCAL}(d_{HCAL})$ is the HCAL central angle (target-HCAL distance), ϵ is the longitudinal polarization of the virtual photon, $E_{e'}$ is the average scattered electron energy, and $E_{p'}$ is the average scattered proton energy.

SBS config.	Q^2 $(GeV/c)^2$	ϵ	E_{beam} (GeV)	θ_{BB} (deg)	d_{BB} (m)	θ_{SBS} (deg)	d_{SBS} (m)	θ_{HCAL} (deg)	d_{HCAL} (m)	$E_{e'}$ (GeV)	$E_{p'}$ (GeV)
4	3.0	0.72	3.73	36.0	1.79	31.9	2.25	31.9	11.0	2.12	2.4
9	4.5	0.51	4.03	49.0	1.55	22.5	2.25	22.0	11.0	1.63	3.2
8	4.5	0.80	5.98	26.5	1.97	29.9	2.25	29.4	11.0	3.58	3.2
14	7.4	0.46	5.97	46.5	1.85	17.3	2.25	17.3	14.0	2.00	4.8
7	9.9	0.50	7.91	40.0	1.85	16.1	2.25	16.0	14.0	2.66	6.1
11	13.6	0.41	9.86	42.0	1.55	13.3	2.25	13.3	14.5	2.67	8.1

Reconstruction Challenges – Looking for Needle in a Haystack!

GEM Layers on a Single Event Display ($Q^2 = 4.5(GeV/c)^2$)

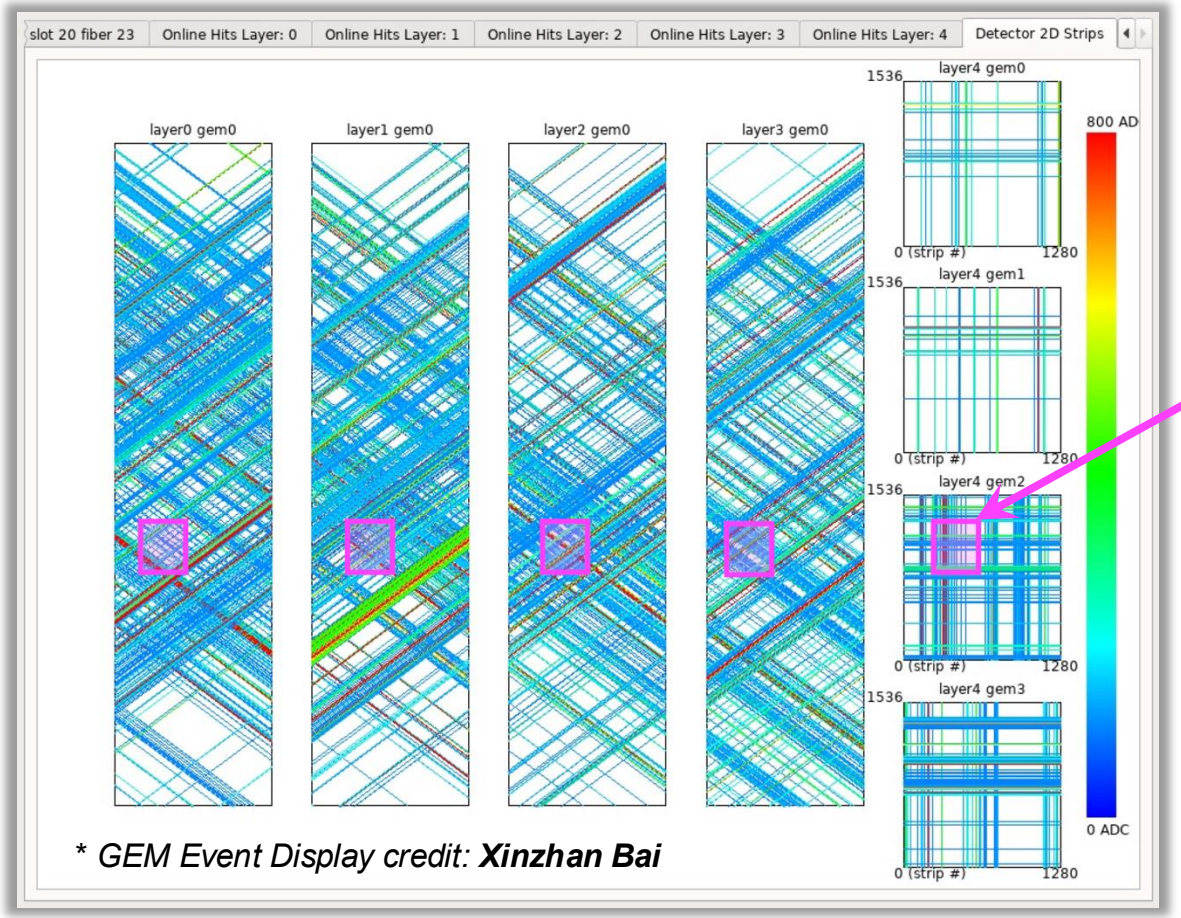

BBCAL constraint

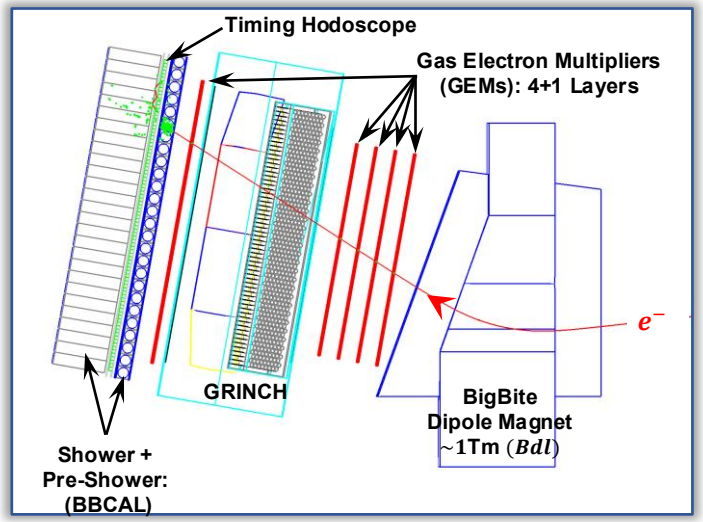

- **Challenge:** Due to very high luminosity number of 2D hit combinatorics can get astronomically high making reconstruction impossible!

- **Remedy:** Define a smaller track search region based on the position of highest energy BBCAL cluster.

- BBCAL constraint reduces the track search region to **2-3**% of the entire GEM active area enabling reconstruction. But it required maintaining excellent gain-matching and calibration of BBCAL during run!

Physics Analysis Methods – Introducing HCAL Δx and Δy

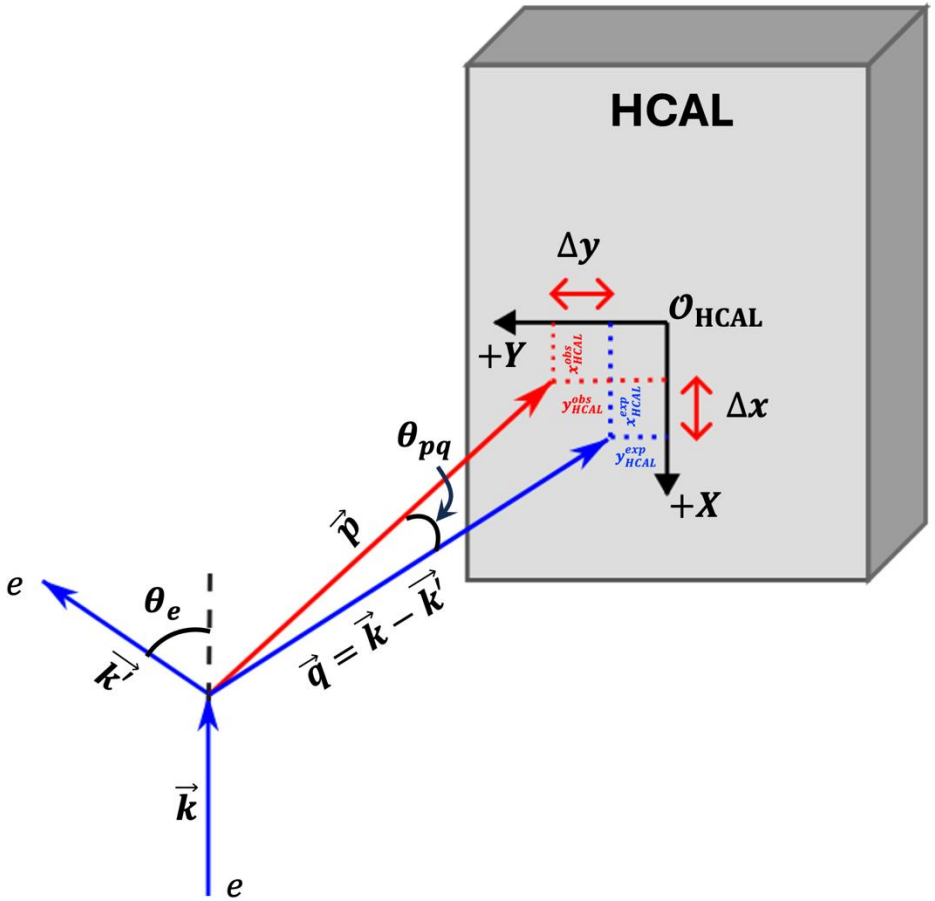

Figure I: A conceptual and exaggerated diagram introducing HCAL Δx and Δy variables. **NOTE:** The presence of the SBS magnet has been **ignored** here.

$\hat{x}$ = Vertical/Dispersive direction

$\hat{y}$ = Transverse direction

- **Definition of Δx:** The difference between the observed (x_{HCAL}^{obs}) and expected (x_{HCAL}^{exp}) nucleon position on HCAL in the vertical (dispersive) direction.

- **Definition of Δy:** The difference between the observed (y_{HCAL}^{obs}) and expected (y_{HCAL}^{exp}) nucleon position on HCAL in the horizontal (non-dispersive) direction.

HCAL Δx and Δy Correlation

Q^2 = 3 $(GeV/c)^2$, SBS 50% Field

Elastic Spot (LH_2 Data)

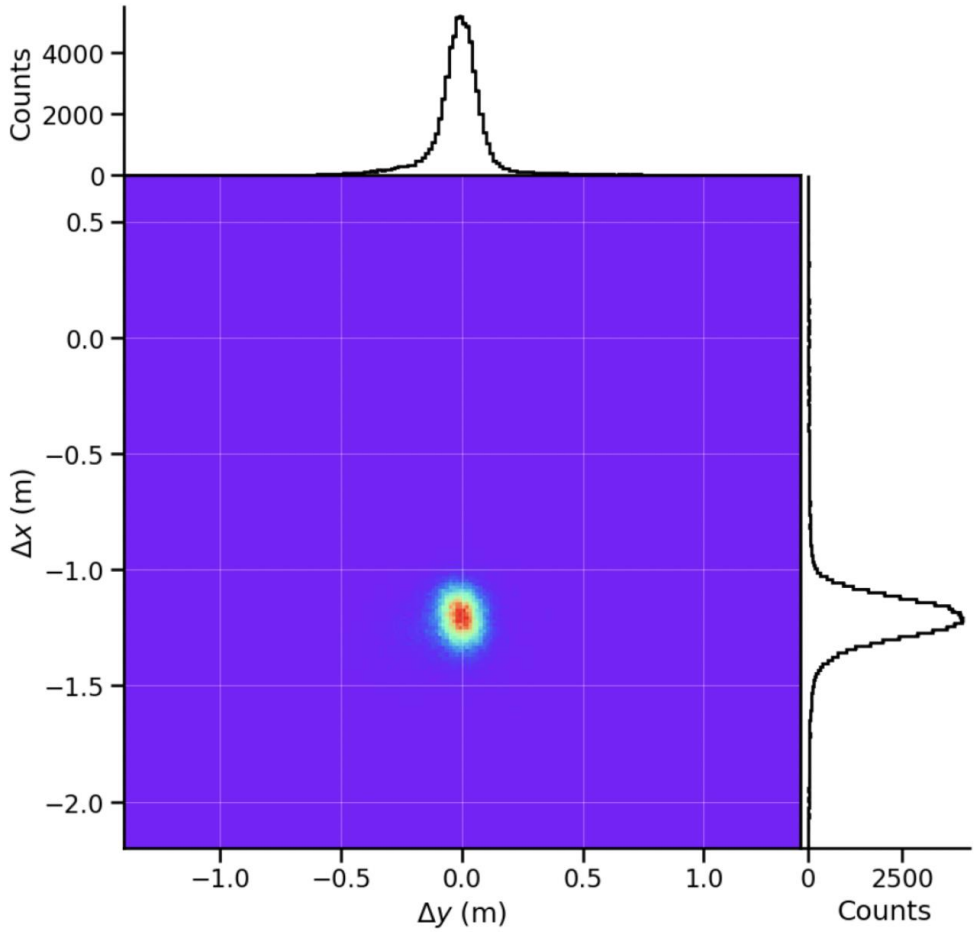

Quasi-Elastic Spots (LD_2 Data)

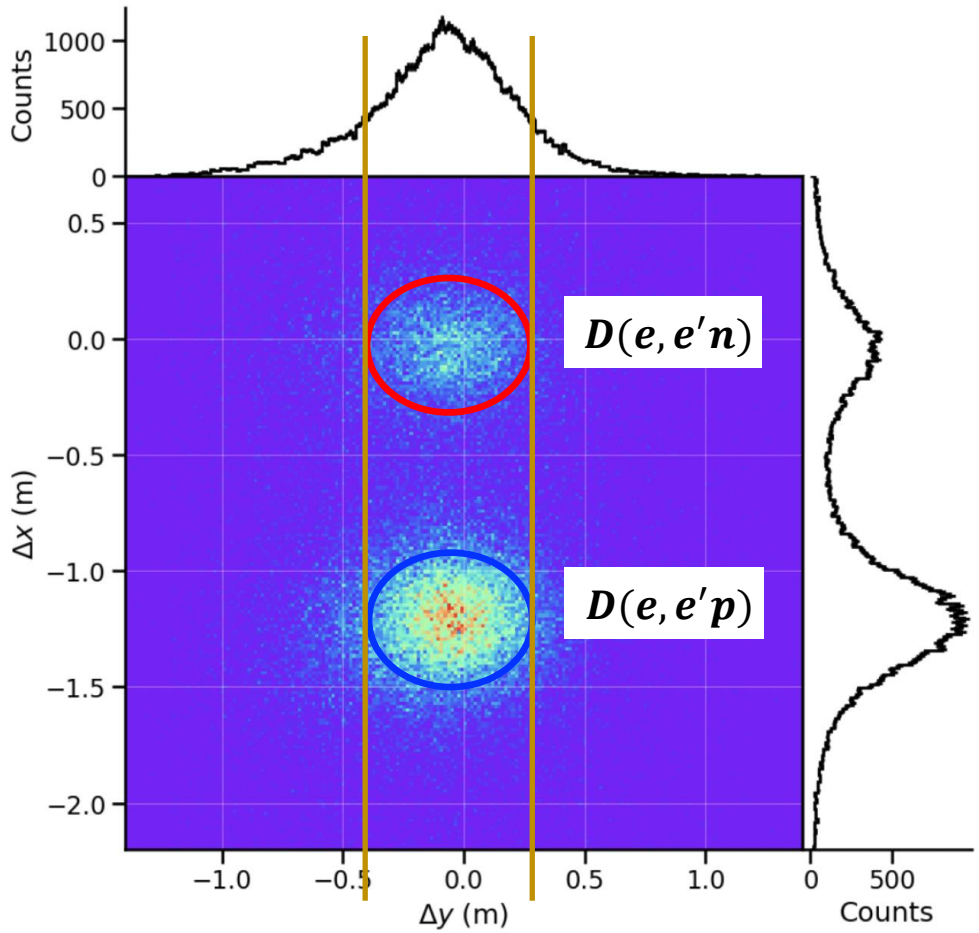

Effects of Analysis Cuts

Q^2 = 3 $(GeV/c)^2$

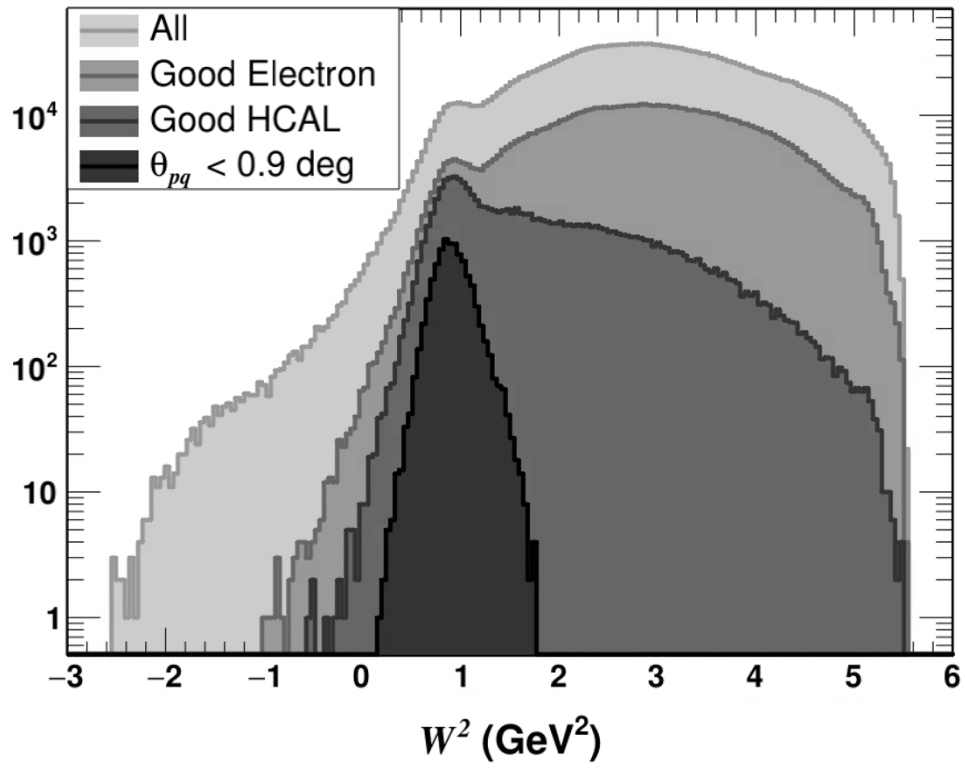

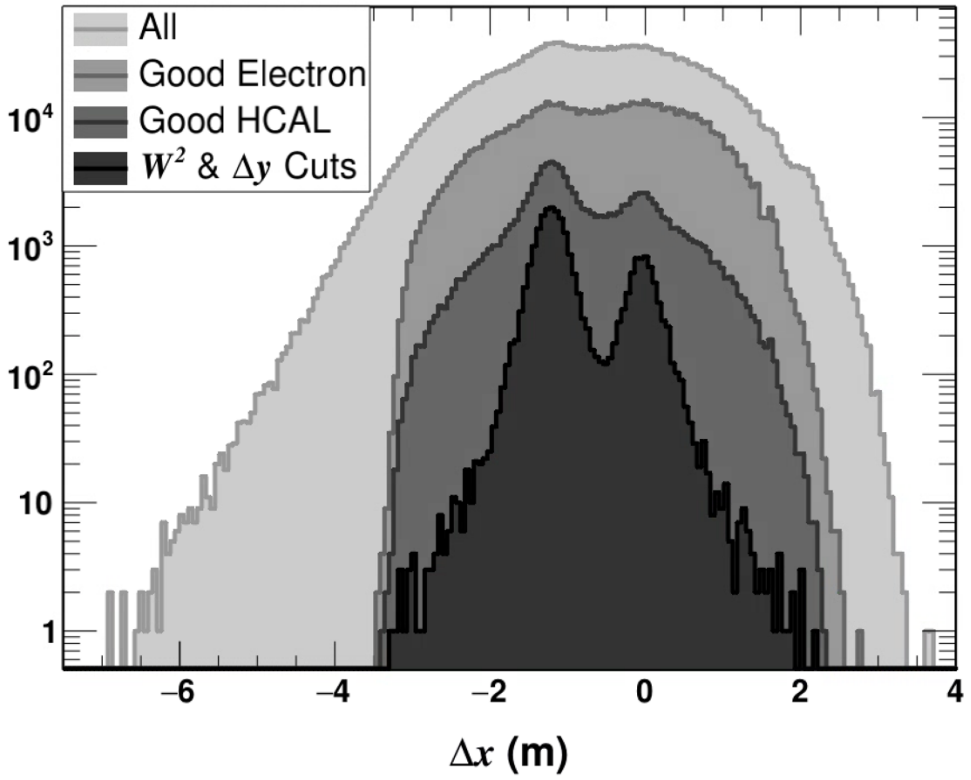

Inclusive W^2

Q^2 = 13.6 $(GeV/c)^2$

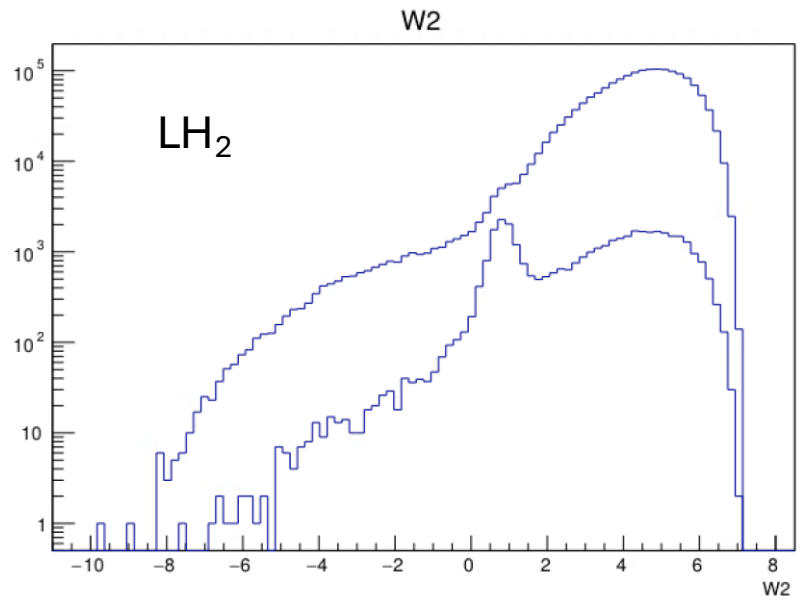

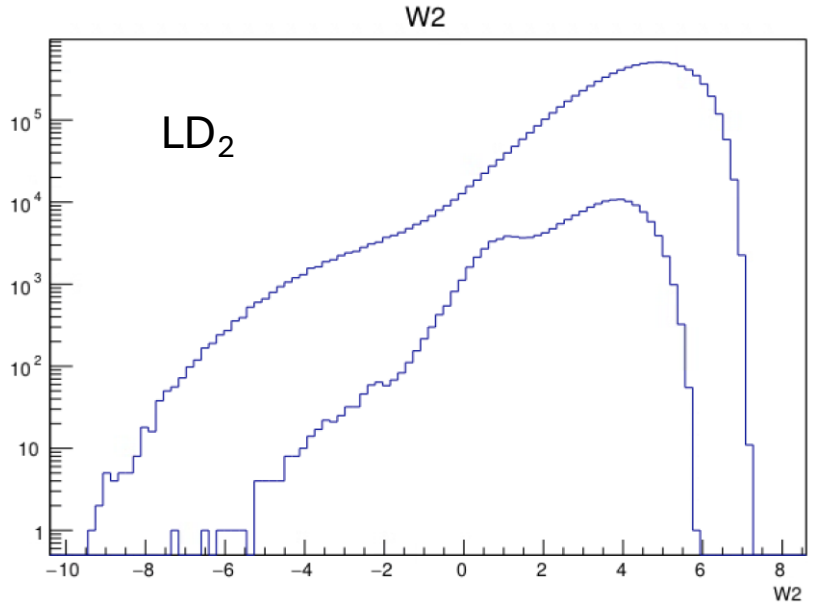

- Inclusive W^2 distribution with and without $\theta_{pq} < 0.6$ deg cut.

Qualitative Data/MC Comparison for $H(e, e'p)$ Events

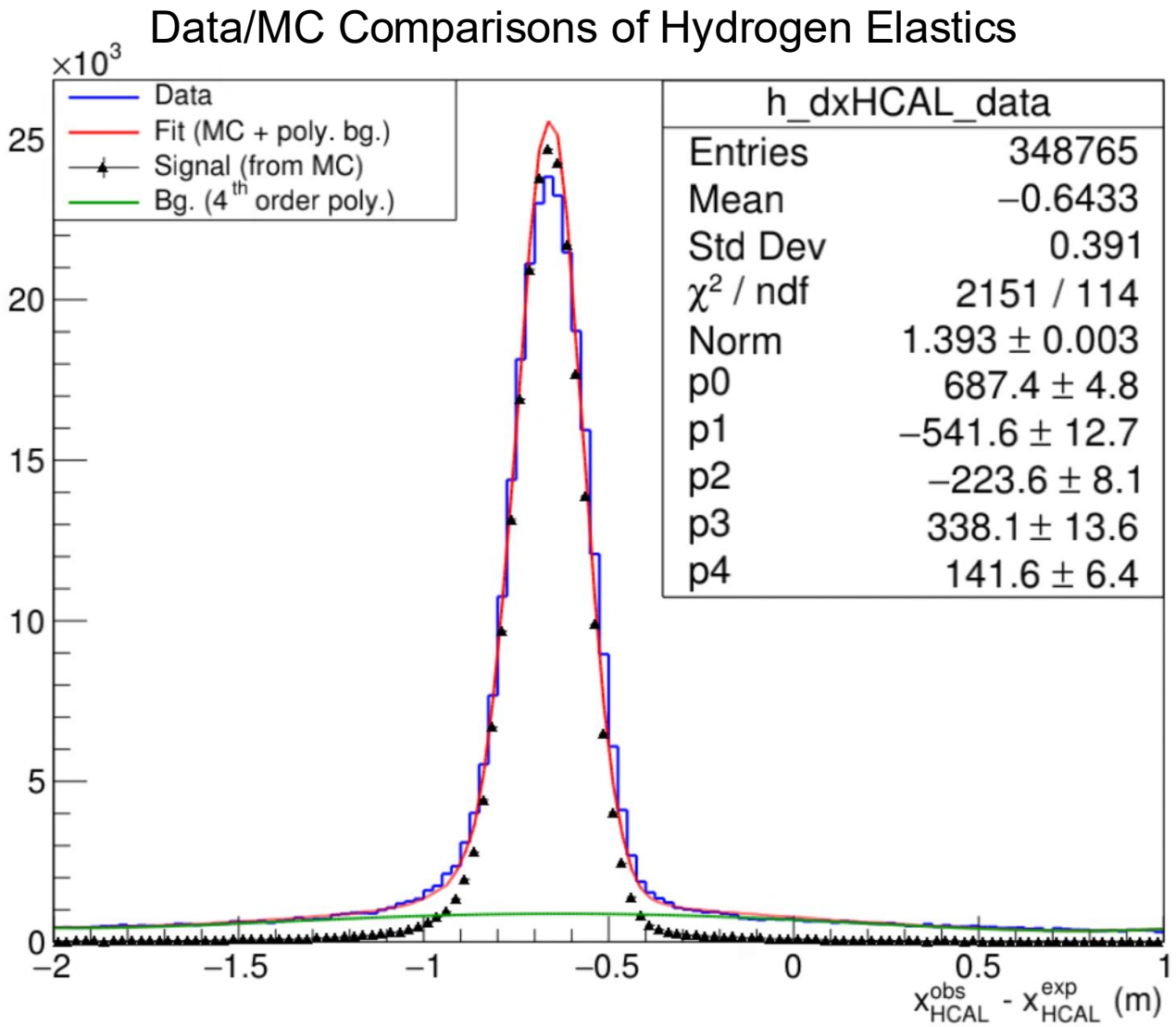

Data/MC Fit to Δx Distribution for Higher Q^2 Points

Q^2 = 9.9 GeV², $0.2 \leq W^2 \leq 1.32$ GeV², Fiducial Cuts

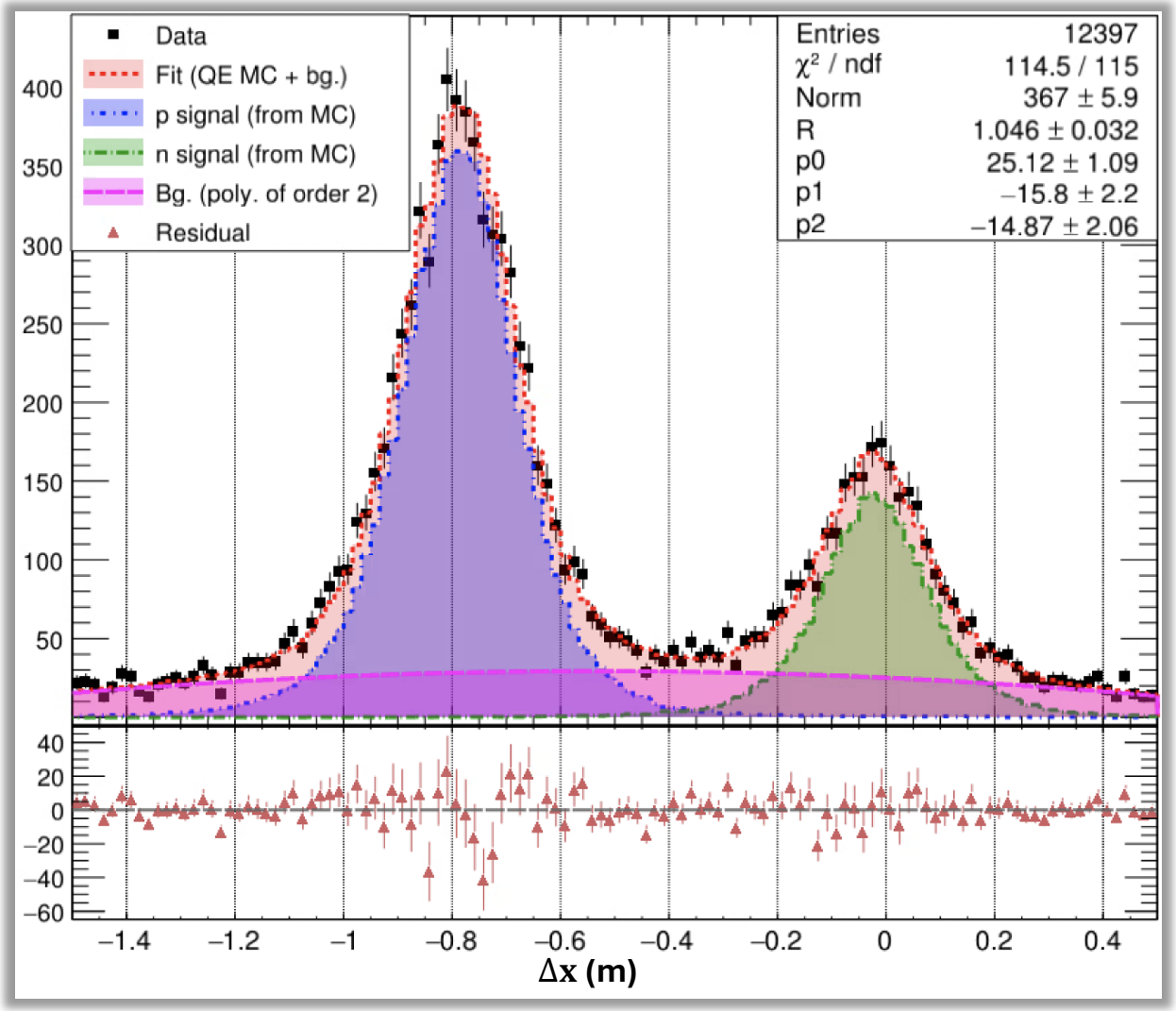

Q^2 = 13.6 GeV², $0.16 \leq W^2 \leq 1.44$ GeV², Fiducial Cuts

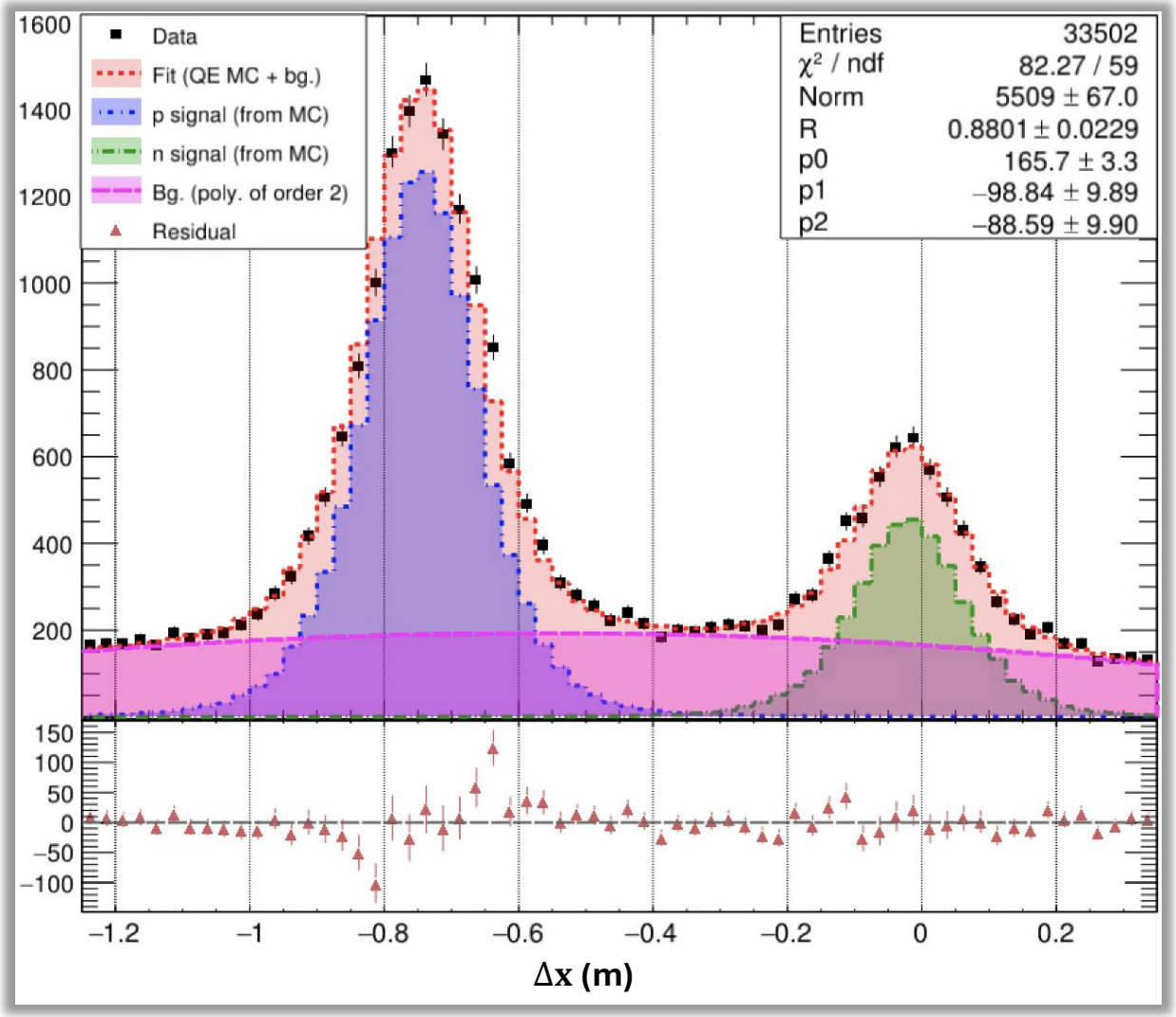

Inelastic Contamination

Q^2 = 7.4 $(GeV/c)^2$

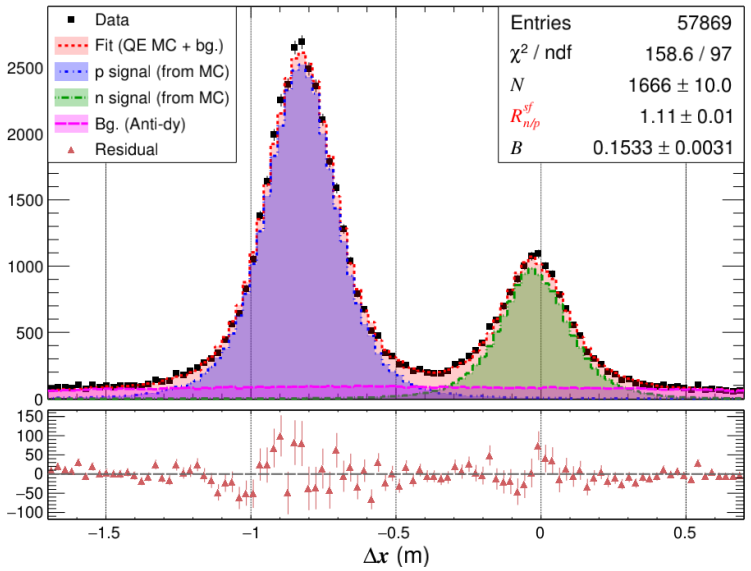

Bg. shape from data

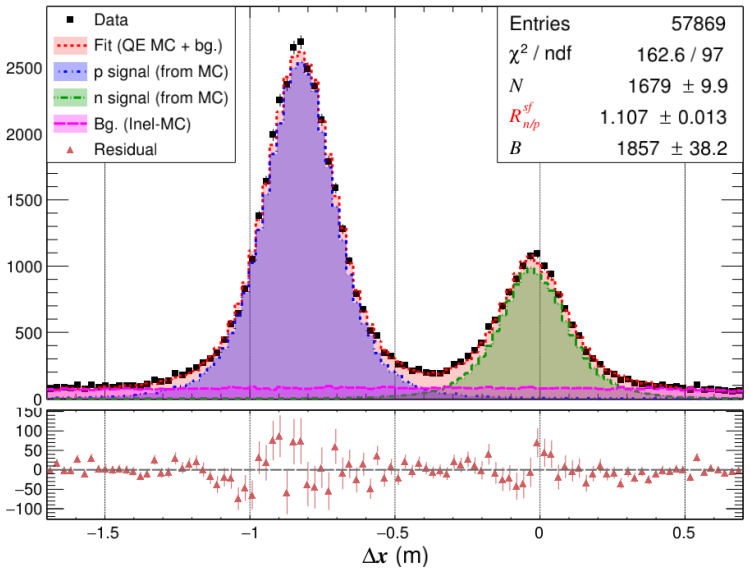

Bg. Shape from Inelastic MC

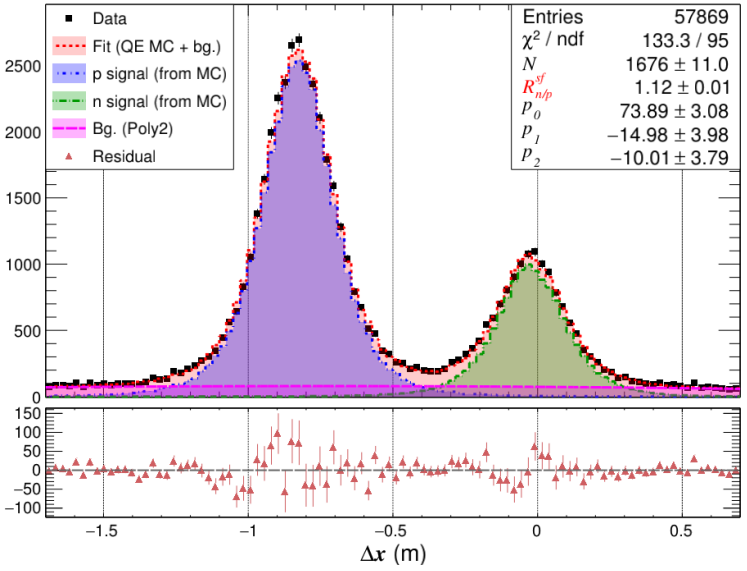

2nd order polynomial

- Perform data/MC fit to Δx distribution using multiple background models.
- Compute standard deviation of $R_{n/p}^{sf}$ values extracted from these fits.
- Quote the result as the systematic uncertainty due to inelastic contamination.

Uncertainty due to Cut Stability

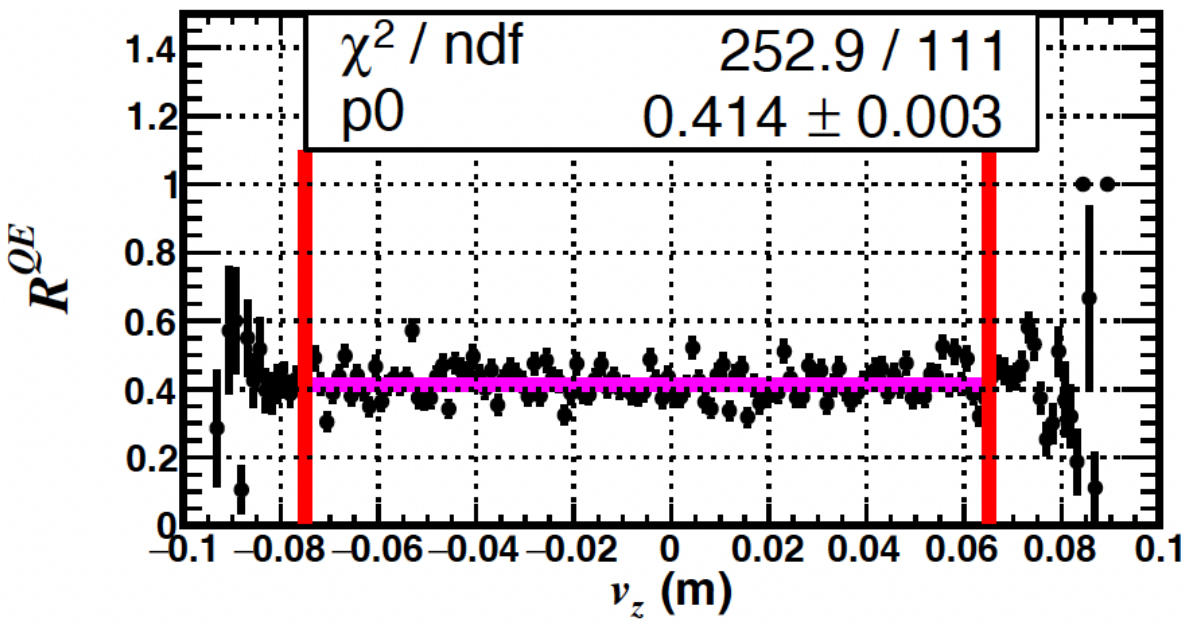

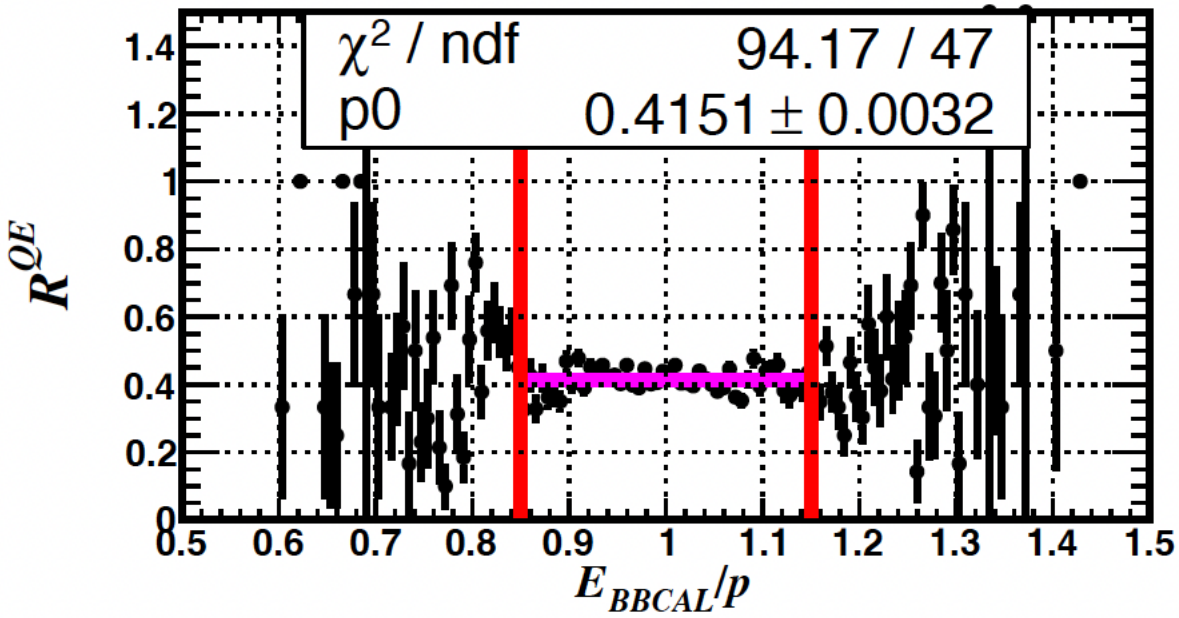

$$R^{QE} = \frac{\frac{d\sigma}{d\Omega}\big|_{D(e,e'n)}}{\frac{d\sigma}{d\Omega}\big|_{D(e,e'p)}}$$

- Stability of $\boldsymbol{R^{QE}}$ vs Cut Variables
- Red vertical lines define the cut region selected based on the stability of R^{QE}.

Cut Stability

- The choice of optimal cut region has some associated uncertainty.
- We vary each cut range by +10% and -10% while keeping the other cuts constant at their optimized values. Then, for each variation extract $R_{n/p}^{sf}$.
- One standard deviation of the resulting $R_{n/p}^{sf}$ distribution is quoted as the associated systematic uncertainty.

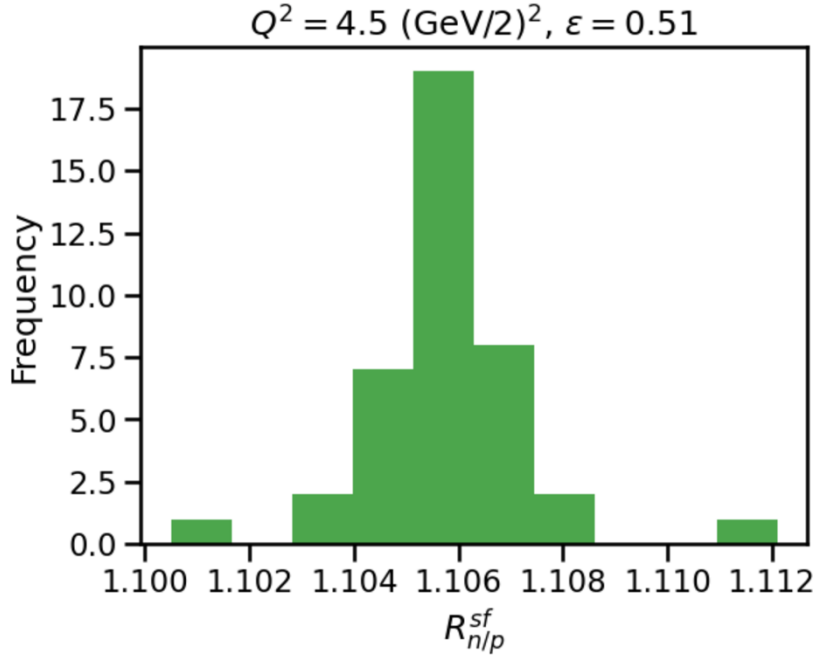

“True” HCAL NDE for MC

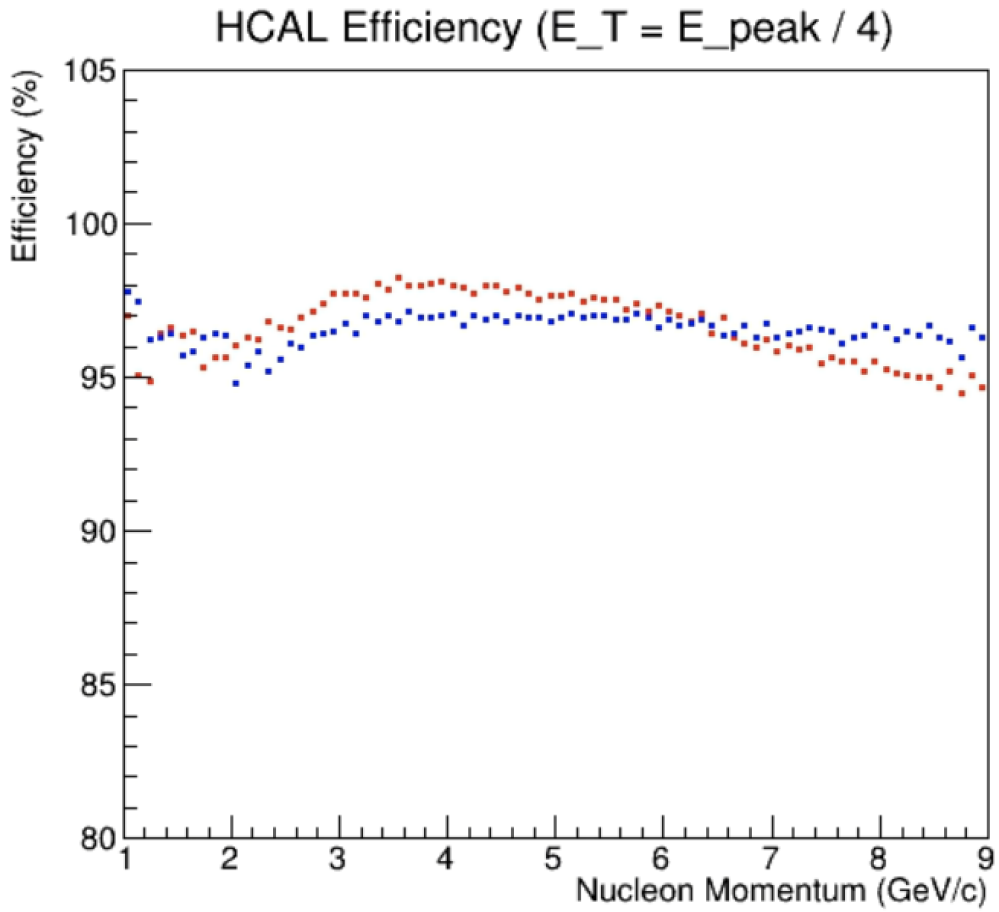

- One of the biggest sources of systematic errors for SBS-GMn/nTPE analysis.
- Very high detection efficiencies, almost independent of nucleon momentum, are expected from simulation.
- MC also show comparable detection efficiencies for proton and neutron, as expected from the design of HCAL.

HCAL pDE – Data/MC Comparison

Dispersive

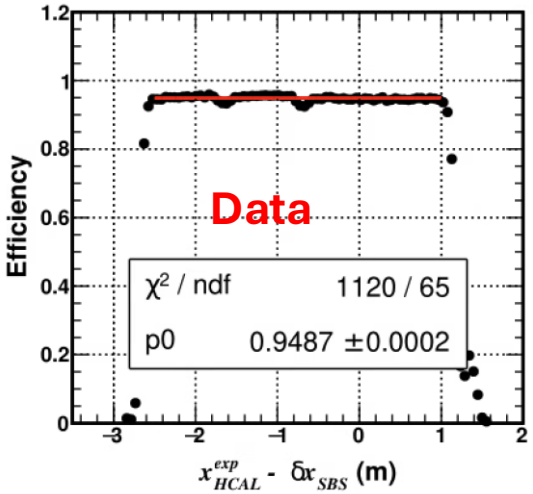

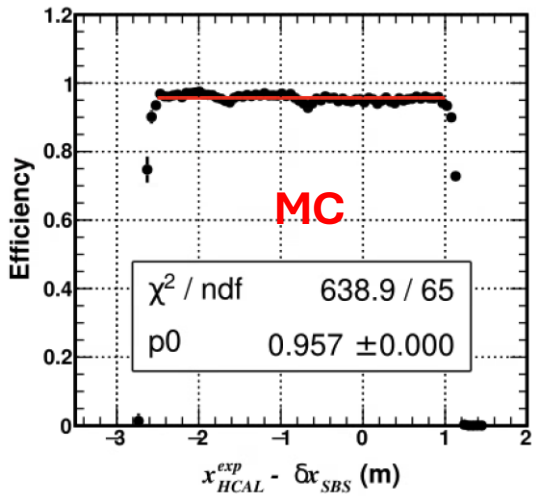

Non-Dispersive

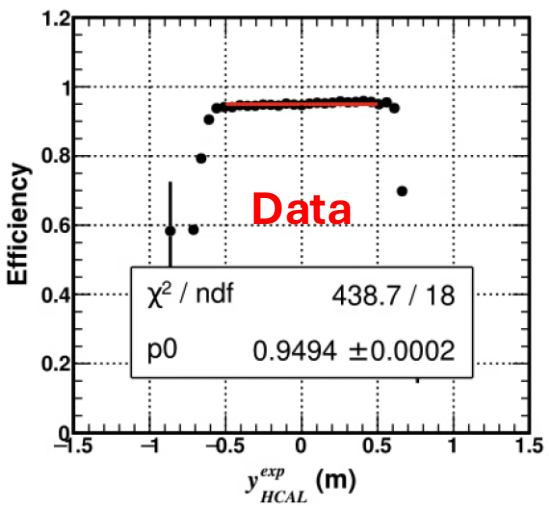

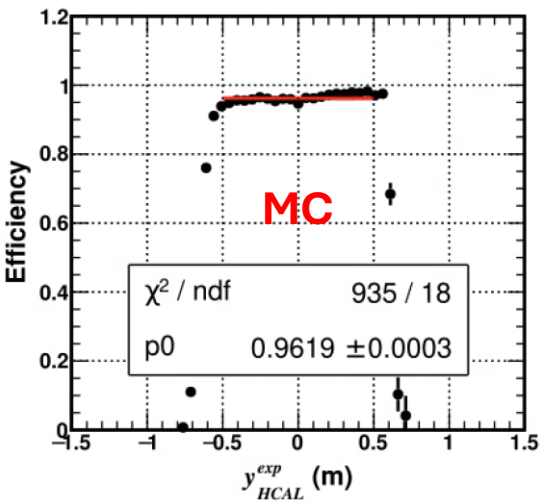

Predicted TPE Contribution

Credit: Andrei Afanasev

E_e GeV	$\theta_{e'}$ deg	Q^2 GeV^2	$(1+\delta)_p$	$(1+\delta)_n$	$(1+\delta)_p/(1+\delta)_n$
3.73	36.0	2.99	1.01809	1.00107	1.01696
4.03	49.0	4.5	1.01746	0.999145	1.01833
5.97	46.5	7.46	1.0202	0.998075	1.02217
7.91	40.0	9.83	1.02168	0.998083	1.02364
9.86	42.0	13.5	1.02242	0.998544	1.02391

Table 1: Table of relevant kinematics in *ep*- and *en*- scattering. The last three columns represent the two-photon corrections for a proton neutron target. The last column is the ratio of the corrections off protons vs neutrons.

Credit: Blunden

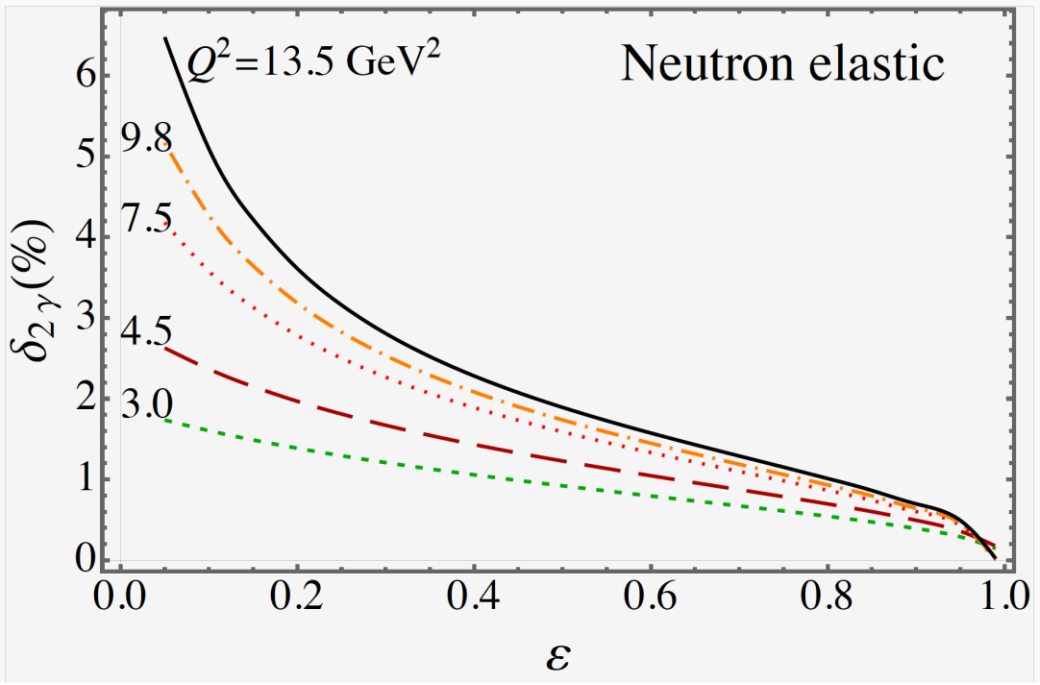

Lattice QCD Calculation of Nucleon Form Factors

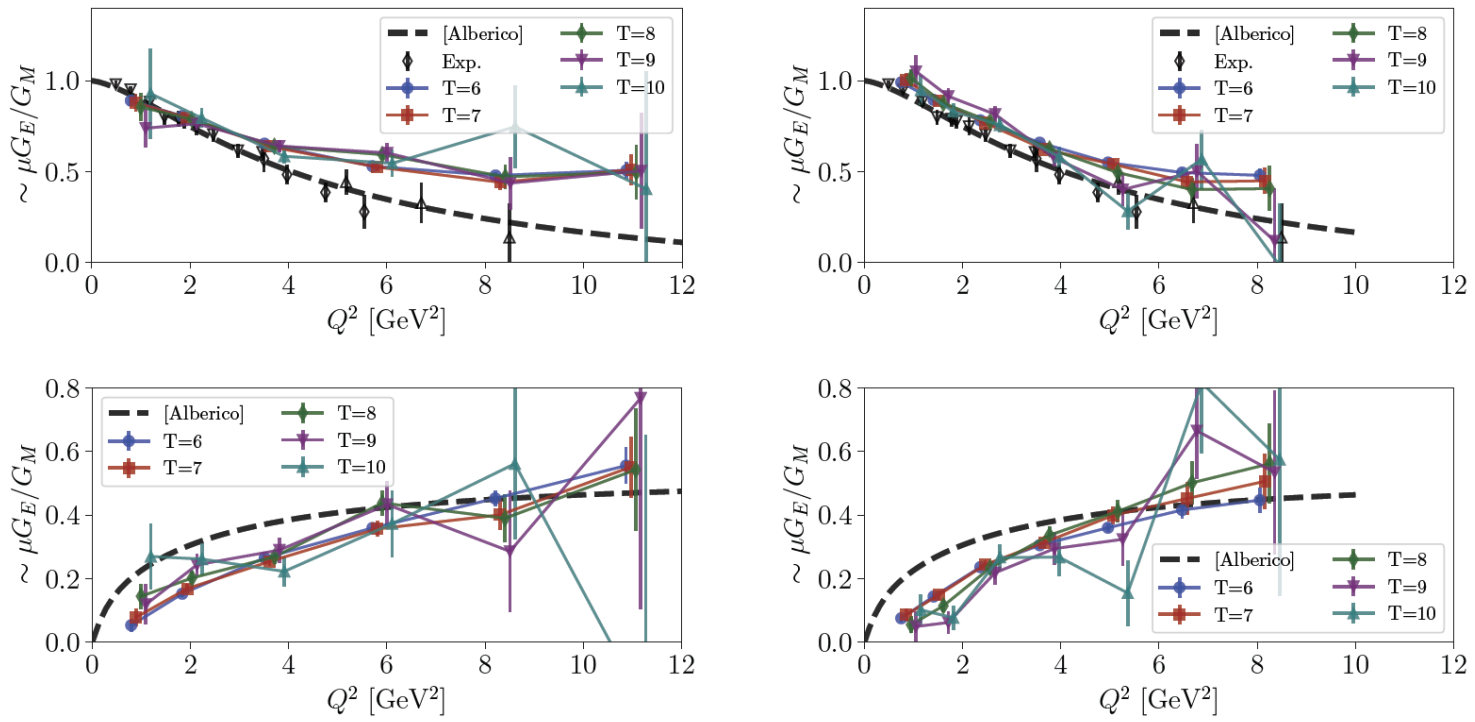

Figure 5: Ratio of the form factors G_E/G_M of the proton (top) and neutron (bottom) on the D5 ($m_\pi \approx$ 280 MeV, left) and D6 ($m_\pi \approx$ 170 MeV, right) ensembles. Both connected and disconnected contributions are included. The black data points are experimental values and the dashed lines are phenomenological fits [17]

In proceedings of LATTICE2024 by S. Syritsyn, M. Engelhardt, S. Krieg, J. Negele and A. Pochinsky arXiv:2502.17283

Impact on the Quark Form Factors (Preliminary)

- Fit Equation:

$$y = p_0(1 + p_1 x)$$

```
****************************************
Minimizer is Minuit2 / Migrad
Chi2                      =      1.37647
NDf                       =            3
Edm                       =  1.08377e-06
NCalls                    =           67
p0                        =     0.623053   +/-   0.0861665
p1                        =    -0.102421   +/-   0.0188333
```

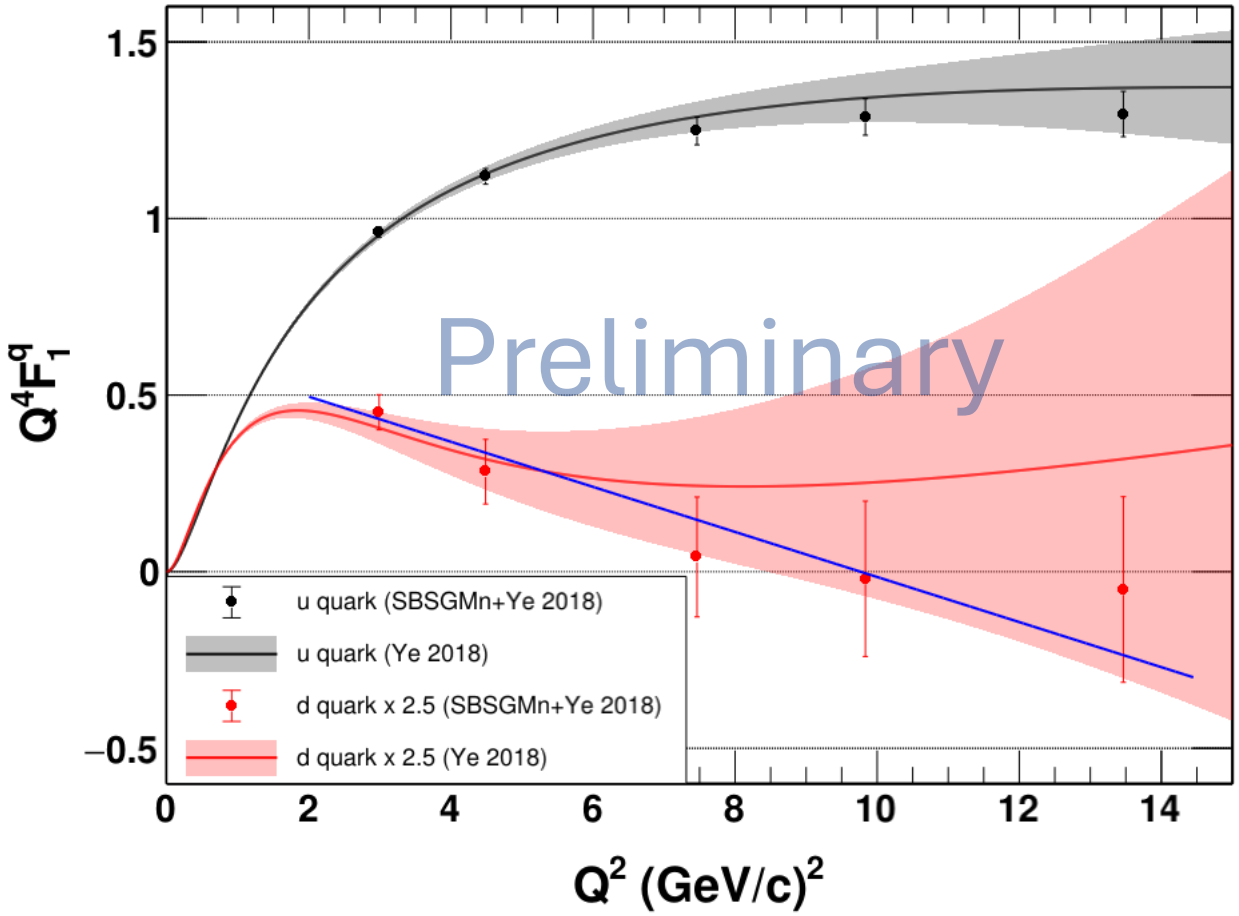

- Possible zero-crossing of $\boldsymbol{F_1^d}$ at $\mathbf{Q^2 = 9.8 \pm 1.8\ (GeV/c)^2}$ (obtained from a linear fit to data).

Impact on the Quark Form Factors (Preliminary) contd.

$$
\begin{aligned}
F_1^d &= 2F_1^n + F_1^p \\
&= 2\frac{\tau_n G_M^n + G_E^n}{1+\tau_n} + \frac{\tau_p G_M^p + G_E^p}{1+\tau_p} \\
&= \frac{2\tau_n}{1+\tau_n} G_M^n + \frac{2}{1+\tau_n} G_E^n + \frac{\tau_p}{1+\tau_p} G_M^p + \frac{1}{1+\tau_p} G_E^p \\
&= G_D \left[\frac{2\tau_n}{1+\tau_n} \frac{G_M^n}{G_D} + \frac{2}{1+\tau_n} \frac{G_E^n}{G_D} + \frac{\tau_p}{1+\tau_p} \frac{G_M^p}{G_D} + \frac{1}{1+\tau_p} \frac{G_E^p}{G_D} \right] \\
&\approx G_D \left[1.6 \frac{G_M^n}{G_D} + 0.4 \frac{G_E^n}{G_D} + 0.8 \frac{G_M^p}{G_D} + 0.2 \frac{G_E^p}{G_D} \right] \\
&\approx G_D \left[(-2.239 \pm 0.085) + (0.249 \pm 0.203) + (1.947 \pm 0.023) + (-0.015 \pm 0.033) \right]
\end{aligned}
$$

For $Q^2 = 13.5\ \mathrm{GeV}^2$

Available Quark Form Factor Predictions

GPD Based Calculation

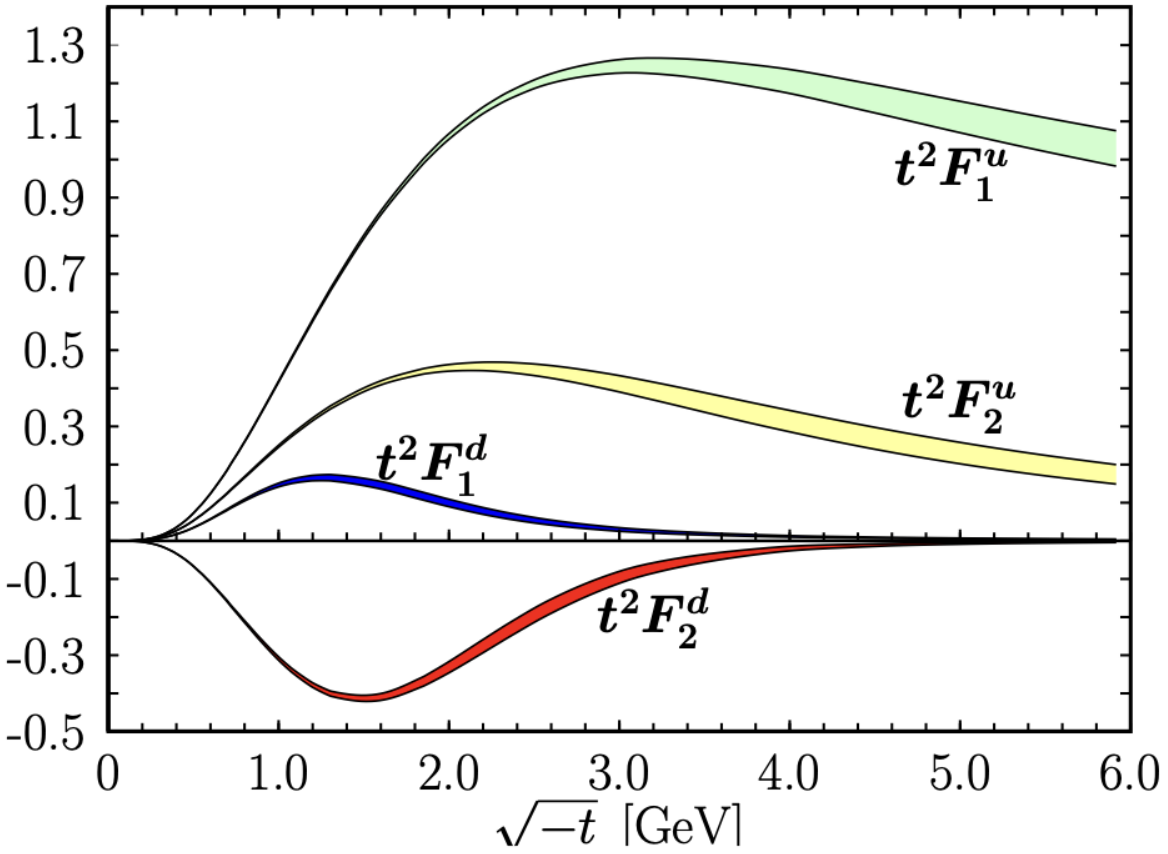

No zero-crossing for F_1^d

Diehl and Kroll, arXiv:1302.4604v1 (2013)

DSE Calculation

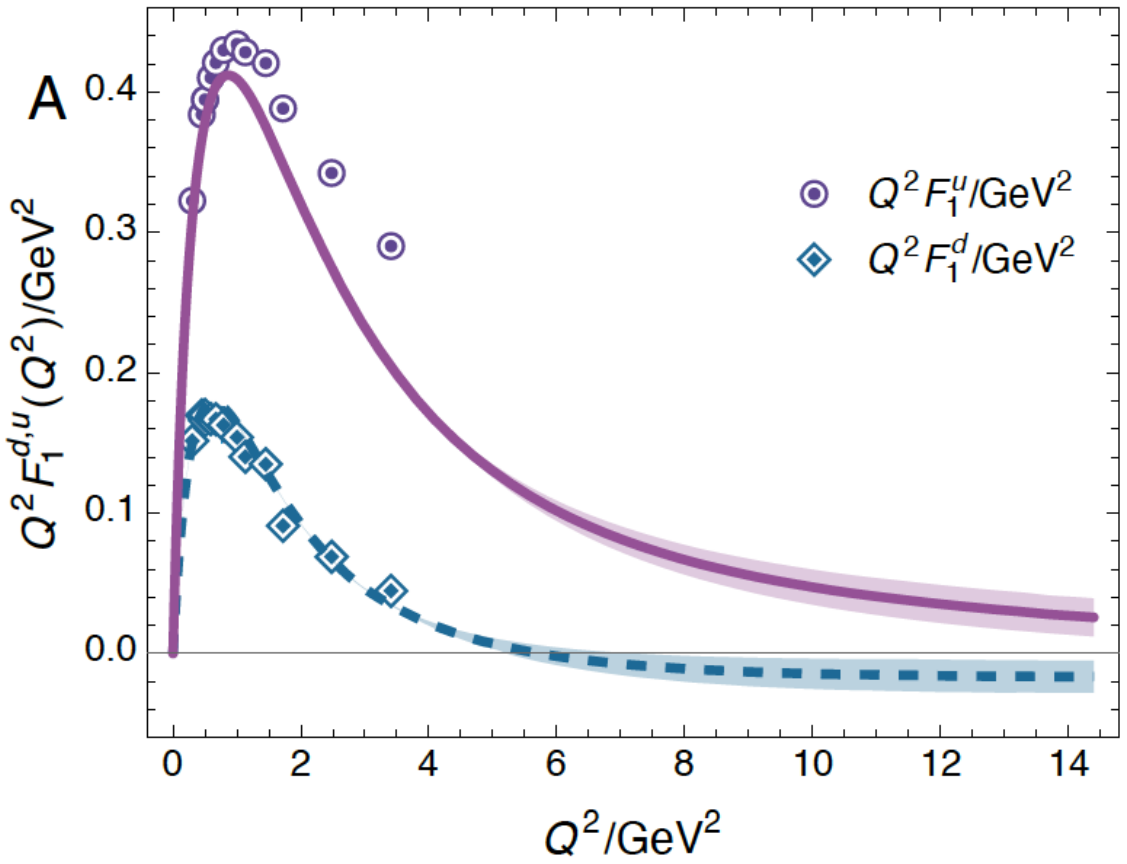

Zero-crossing for F_1^d at around 6 $(\mathrm{GeV}/c)^2$

Yao et al, https://doi.org/10.1016/j.fmre.2024.11.005 (2024)